## FIGURE CAPTIONS

**Fig. 1.1**

Location map of the Japan Trench area and its three sub-regions.

**Fig. 1.2**

Summary of large offshore earthquakes along the Japan Trench (1885 - 1980). Rupture zones of some of the earthquakes are also shown by enclosed areas. Reproduced from Kawakatsu and Seno (1983).

**Fig. 1.3**

Epicenter distribution in the Japan Trench area determined by the microearthquake network of Tohoku University. Reproduced from Faculty of Science, Tohoku University (1983).

**Fig. 1.4**

Locations of refraction survey lines conducted in the Japan Trench area (solid and broken lines). The broken line corresponds to the profile of Asano *et al.* (1981) which is not reversed. The shaded line is the refraction line of this study.

**Fig. 1.5**

P-wave velocity structure section across the Japan Trench in Sanriku-Oki compiled by Kanazawa *et al.* (1985).

**Fig. 3.1**

Hardware block diagram of the minicomputer system. Units with stars were introduced after Urabe and Hirata (1984)'s system was

developed.

**Fig. 3.2**

An example of rectified and low-pass filtered seismic signal used for event detection. (a): Original waveform. (b): Output from the signal conditioning unit.

**Fig. 3.3**

An example of restored (square-shaped) time code signal. (a): Original waveform. (b): Output from the signal conditioning unit.

**Fig. 3.4**

(A) An example of the event list produced by the program "EVDET". Each line corresponds to a seismic event. (1): event number, (2): time (day, hour, minute, second), (3): duration (s), (4): maximum amplitude, (5): integration of amplitude, (6): ID number of the time code generator, (7): sampling rate (Hz), (8): LTA at the trigger, (9): and (10): the block and data address of the trigger point in the file.

(B) An example of the filing schedule table used for the program "AUTO". Each line corresponds to a record to be digitized. (1): time (day, hour, minute, second), (2): time length (s), (3): gain index for the A/D converter.

(C) Examples of record headers. Each line corresponds to a record. (1): event number, (2): time (in days, hours, minutes, s and ms, respectively), (3): sampling rate (Hz), (4): amplitude resolution at digitizing ($\mu$V), (5): block address in the file,

(6): number of blocks occupying, (7): number of data in the last block, (8): ID number of the time code generator, (9): polarity of the time code signal, (10): difference between actually digitized and scheduled times (s).

**Fig. 3.5**

**Method of compiling event lists made from single stations into a filing schedule common to the network. Event periods in the** lists are extended backward and forward by $T_{pre}$ and $T_{post}$, respectively. If the number of stations simultaneously in the extended event period is no less than a specified number $N_{min}$ (during a period $T_a$), the period just inclusive of all the extended event periods ($T_b$) is decided for a synthesized event period, and then it is added to the filing schedule table.

**Fig. 3.6**

Flow diagram of the system. In quotation marks are names of programs. The whole series of procedures in the middle was introduced for the improved version.

**Fig. 4.1**

Location map of the experiments. Isobaths are in meters. The OBSs of the 1982 experiment are designated by squares and those of the 1985 experiment are by circles and triangles. OBS S1 (open triangle) was lost. The broken line corresponds to the seismic refraction survey line. The earthquake network of the 1985 experiment consisted of the OBSs designated by circles.

**Fig. 4.2**

Daily number of events detected by each OBS of the 1982 array. High rates in the middle of the observation period are related to the occurrence of the 1982 Ibaraki-Oki earthquake ($M$ = 7.0) at 100 km south of the array.

**Fig. 4.3**

An example of seismogram obtained with the 1982 array in the multi-station format. Station's name and signal component are marked on the left of each trace. A coded clock signal is at the top. *P* and *S* phases are designated by downward arrowheads and *PS* converted phases are by upward ones.

**Fig. 4.4**

Observation period of each OBS in the 1985 experiment. OBS names are on the left. An OBS pair having the same number in their names mean replacement at the same location. The lower 6 OBSs formed the earthquake network.

**Fig. 4.5**

Record sections of OBS S2. Distance along the profile is referred to the OBS position and is positive southward. Reduction velocity is 7.0 km/s. (A): Vertical component, high-gain channel. Pass-band of filtering is 3 - 20 Hz. Amplitude of background noise is normalized for each trace to enhance the first arrivals. (B): The same as (A), but for low-gain channel. (C): Vertical component, low-gain channel. Pass-band of filtering is 3 - 10 Hz. Amplitude is boosted in proportion to

the cube of epicentral distance for the shots farther than 60 km.

**Fig. 4.6**

The same as Fig. 4.5, but for OBS P3/PR3.

**Fig. 4.7**

The same as Fig. 4.5, but for OBS S4.

**Fig. 4.8**

**The same as Fig. 4.5, but for OBS P5/PR5.**

**Fig. 4.9**

The same as Fig. 4.5, but for OBS S6.

**Fig. 4.10**

The same as Fig. 4.5, but for OBS P7/PR7.

**Fig. 4.11**

The same as Fig. 4.5, but for OBS S9.

**Fig. 4.12**

The same as Fig. 4.5, but for OBS S10.

**Fig. 4.13**

Daily number of events detected by each OBS of the 1985 array. High rates in the first half of the observation period in OBS P11 are due to high noise levels.

**Fig. 4.14**

Examples of the multi-station monitor records used in event discrimination. Names of OBSs are marked on the left. **(A)**: An

example of a local microearthquake. *P* and *S* phases are recognized in some stations. (B): An example of a distant earthquake. *P* and *S* phases are easily recognized. (C): An example of *T* phases or water waves of distant earthquakes. Although they look like having *P* and *S* phases, their apparent velocities are too slow to be other than water waves.

**Fig. 4.15**

An example of the multi-station seismogram obtained with the 1985 array. OBS name, component and channel are marked on each trace. *P* and *S* phases are designated by downward arrows and *PS* converted phases are by upward ones. Note that a wide dynamic range of the upper 3 OBSs facilitated pickings of *S* phases in the horizontal component without saturation.

**Fig. 5.1**

Comparison of structure models obtained with the slope-intercept method from a complete and reduced data sets. A: The model obtained from the complete data set with 0.25 s-spaced intercept times. B: One obtained from a subset in which the first (uppermost) crustal slope-intercept data pair is omitted. C: One obtained from a subset in which the last (lowermost) crustal data pair is omitted. D: One obtained from a subset in which every second data pair is omitted.

**Fig. 5.2**

One-dimensional structure models of P-wave velocity obtained for each single sided profile with the slope-intercept analysis.

Station code is written on the upper-left of each diagram. Solid and broken lines correspond to the models derived from the records of the northward and southward shots, respectively.

**Fig. 5.3**

The final P-wave velocity structure model obtained through ray-tracing. Triangles denote the positions of OBSs. Distance along the profile is measured from OBS S10 southward.

**Fig. 5.4**

Ray diagrams in ray-tracing of the final model for three representative OBSs S2 (top), S6 (middle) and S10 (bottom). Distance along the profile is measured from OBS S10 southward.

**Fig. 5.5**

Record section, observed and calculated travel times, and synthetic seismograms for OBS S2. Distance ($D$) is referred to the position of OBS S10, the northern end of the profile. OBS is at $D$ = 174.7 km. **(Top)**: Record section of low-gain channel of vertical component. A band-pass filter (3 - 10 Hz) is applied and amplitudes are boosted by the cube of the epicentral distance for the shots farther than 60 km. **(Middle)**: Plots of picked travel times (solid circles) and those of calculated ones for the final model (other symbols). In the shorter epicentral range, the name of the phase (*PmP*) or the name of the layer which reflected the rays at its top is denoted for each reflected phase. In the longer range, the name of the phase ($P_n$) or the name of the layer within which the rays turn up are marked for

each diving phase. Direct water waves are not calculated. **(Bottom)**: Synthetic record section for the final model.

**Fig. 5.6**

The same as Fig. 5.5, but for OBS P3/PR3. OBS is at $D$ = 153.6 km.

**Fig. 5.7**

**The same as Fig. 5.5, but for OBS S4. OBS is at $D$ = 139.7 km.**

**Fig. 5.8**

The same as Fig. 5.5, but for OBS P5/PR5. OBS is at $D$ = 125.0 km.

**Fig. 5.9**

**The same as Fig. 5.5, but for OBS S6. OBS is at $D$ = 101.6 km.**

**Fig. 5.10**

The same as Fig. 5.5, but for OBS P7/PR7. OBS is at $D$ = 74.1 km.

**Fig. 5.11**

The same as Fig. 5.5, but for OBS S9. OBS is at $D$ = 27.7 km.

**Fig. 5.12**

The same as Fig. 5.5, but for OBS S10. OBS is at $D$ = 0.0 km.

**Fig. 5.13**

P-wave velocity structure model used in the hypocenter location (solid lines). Models between those indicated by broken lines were also tried (see also Fig. 5.14).

**Fig. 5.14**

Relation between the depth of the Moho of structure models and the travel time residuals (*O-C* times) which are normalized by the corresponding reading accuracy and averaged over all data. Circles and triangles denote P and S data, respectively.

**Fig. 5.15**

Epicenters located (solid circles). Number of events are 303 (147 from 1982 and 218 from 1985). OBS arrays are denoted by crosses (OBSs) and connected by broken lines.

**Fig. 5.16**

Hypocenters determined in the observation in 1982. Hypocenters and OBSs are denoted by circles and crosses, respectively. Events with errors less than 10 km are plotted. Number of events are 123. **Upper**: Horizontal distribution. Isobaths are in kilometers. **Lower**: vertical section right across the trench (viewed from S 25 $^{o}$W). "T.A." stands for the trench axis.

**Fig. 5.17**

The same as Fig. 5.16, but the hypocenters are represented by error ellipses.

**Fig. 5.18**

The same as Fig. 5.16, but for the observation in 1985. Number of events are 72.

**Fig. 5.19**

The same as Fig. 5.18, but the hypocenters are represented by error ellipses.

**Fig. 5.20**

Relation between the stations-averaged *F-P* times and $M_{JMA}$. Circles and triangles denote the events of the 1982 and the 1985 experiments, respectively. *F-P* times are those measured automatically with the *STA/LTA* method with different parameter settings for 1982 and 1985.

**Fig. 5.21**

Magnitude - frequency relations for the earthquake observations in 1982 (left) and 1985 (right). The area of epicenters are 36.5 - 38.0 $^{o}$N and 141.0 - 144.0 $^{o}$E.

**Fig. 5.22**

Epicenter distributions determined by the land-based microearthquake network during July, 1982 (upper; Faculty of Science, 1983) and October, 1985 (lower; Faculty of Science, Tohoku University, 1986). Corresponding OBS network of this study is superposed on each map.

**Fig. 6.1**

Crust and uppermost mantle structure and free air gravity anomaly along the Japan Trench measured on its landward slope. Top: Locations of three refraction lines (thick bars); from north to south (left to right), Sanriku-Oki (Kanazawa *et al.*, 1985), Fukushima-Oki (this study) and Boso-Oki (Kanazawa *et al.*, 1985) profiles. Note that the north is to the left. Isobaths are in

kilometers. The 3.5 km isobath is exceptionally designated by a broken line. Areas deeper than 7 km are shaded. **(a)**: Compilation of the results of the three refraction profiles. **(b)**: Free air gravity anomaly just along the 3.5 km isobath which is designated in the location map above. Free air gravity anomaly and bottom topography data were taken from Tomoda and Fujimoto (1982).

**Fig. 6.2**

Bathymetric chart of the Northwestern Pacific. Isobaths are in kilometers with intervals of 1 km, except for those of 5.5 km designated by broken curves. Isobaths in the area shallower than 5.0 km are omitted for simplicity.

**Fig. 6.3**

Water depth profile along the lines parallel to the Japan Trench axis on its ocean side. The Number attached to each line in the figure indicates the distance from the trench axis in degrees of longitude. One degree equals about 90 km in these latitudes. The water depth data were taken from Tomoda and Fujimoto (1982).

**Fig. 6.4**

Geomagnetic anomaly in the Northwest Pacific. **(a)**: Mesozoic magnetic anomaly lineations identified by Hilde *et al.* (1976). Anomaly Nos. 10 - 20 correspond approximately to 130 - 150 m.y.B.P. **(b)**: Recently published geomagnetic anomaly map based on more data than the above (Isezaki, 1987).

**Fig. 6.5**

Comparison of two vertical sections of hypocenter distribution across the Japan Trench obtained with OBS arrays. **Upper**: Sanriku-Oki (38 - 41 $^{o}$N) obtained by Yamada (1980) and Hirata *et al.* (1983 and 1985). **Lower**: Fukushima-Oki (36.5 - 38.0 $^{o}$N). Different symbols designate different observations as denoted above each section. The ranges of the OBS arrays are also shown. Dotted curves designate the positions of the top of the 8 km/s layer (uppermost mantle) in the subducting oceanic plate assumed from the refraction experiments.

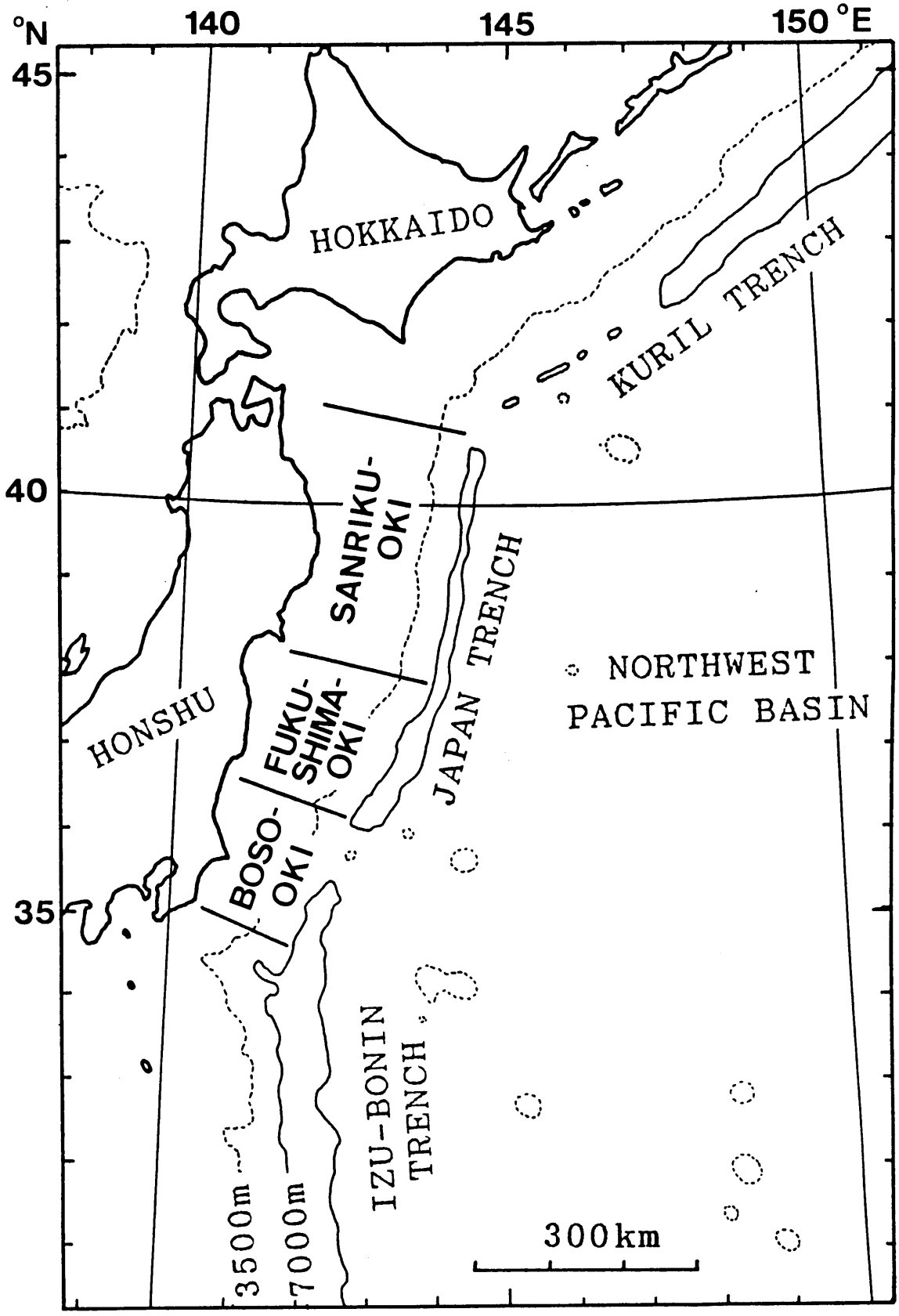
°N
140
145
150 °E
45
40
35
HOKKAIDO
KURIL TRENCH
SANRIKU-OKI
JAPAN TRENCH
NORTHWEST PACIFIC BASIN
HONSHU
FUKU-SHIMA-OKI
BOSO-OKI
IZU-BONIN TRENCH
3500m
7000m
300km

FIG. 1.1

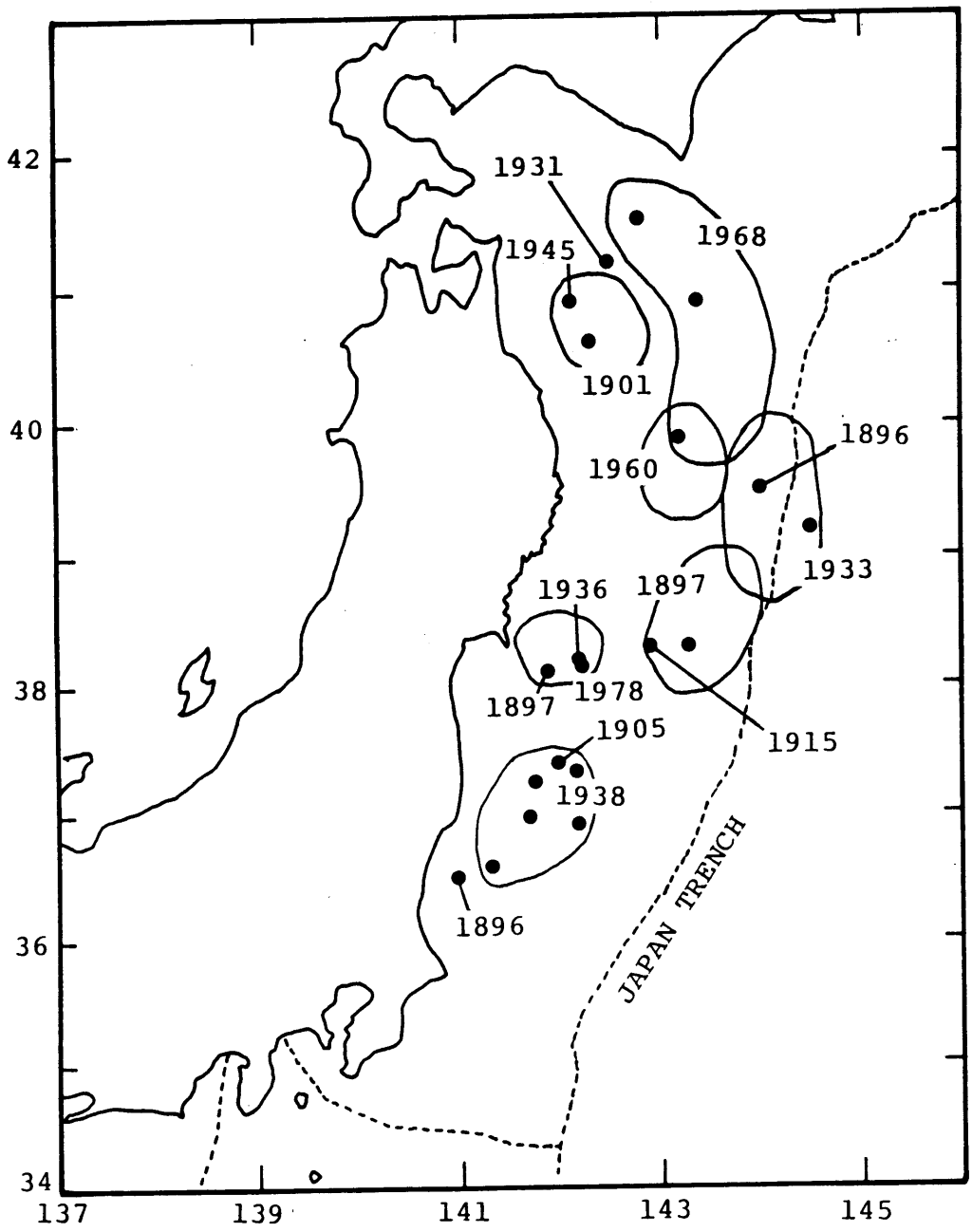
42
40
38
36
34
137
139
141
143
145
1931
1945
1968
1901
1896
1960
1933
1936
1897
1978
1897
1905
1915
1938
1896
JAPAN TRENCH

FIG. 1.2

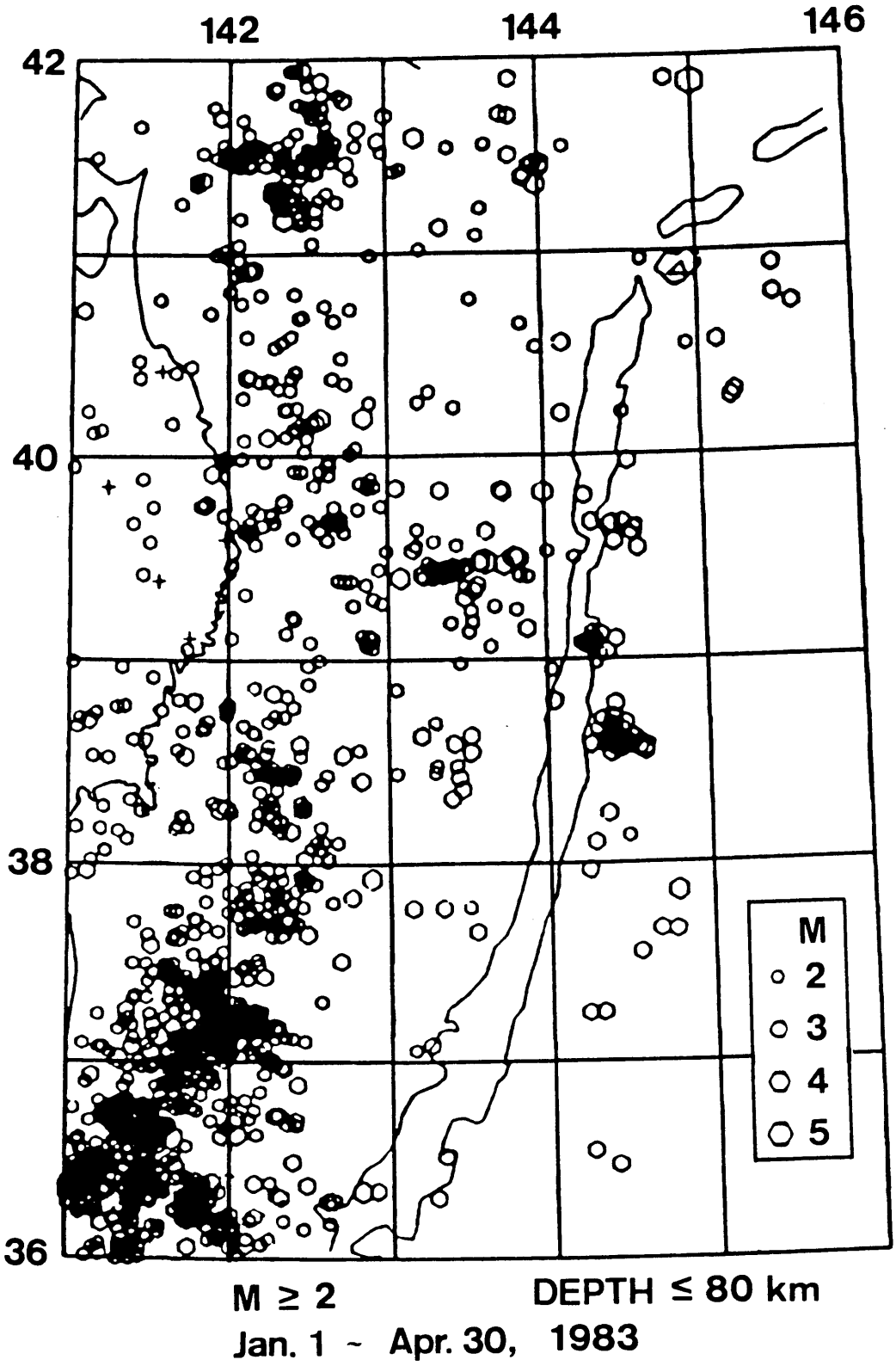


FIG. 1.3

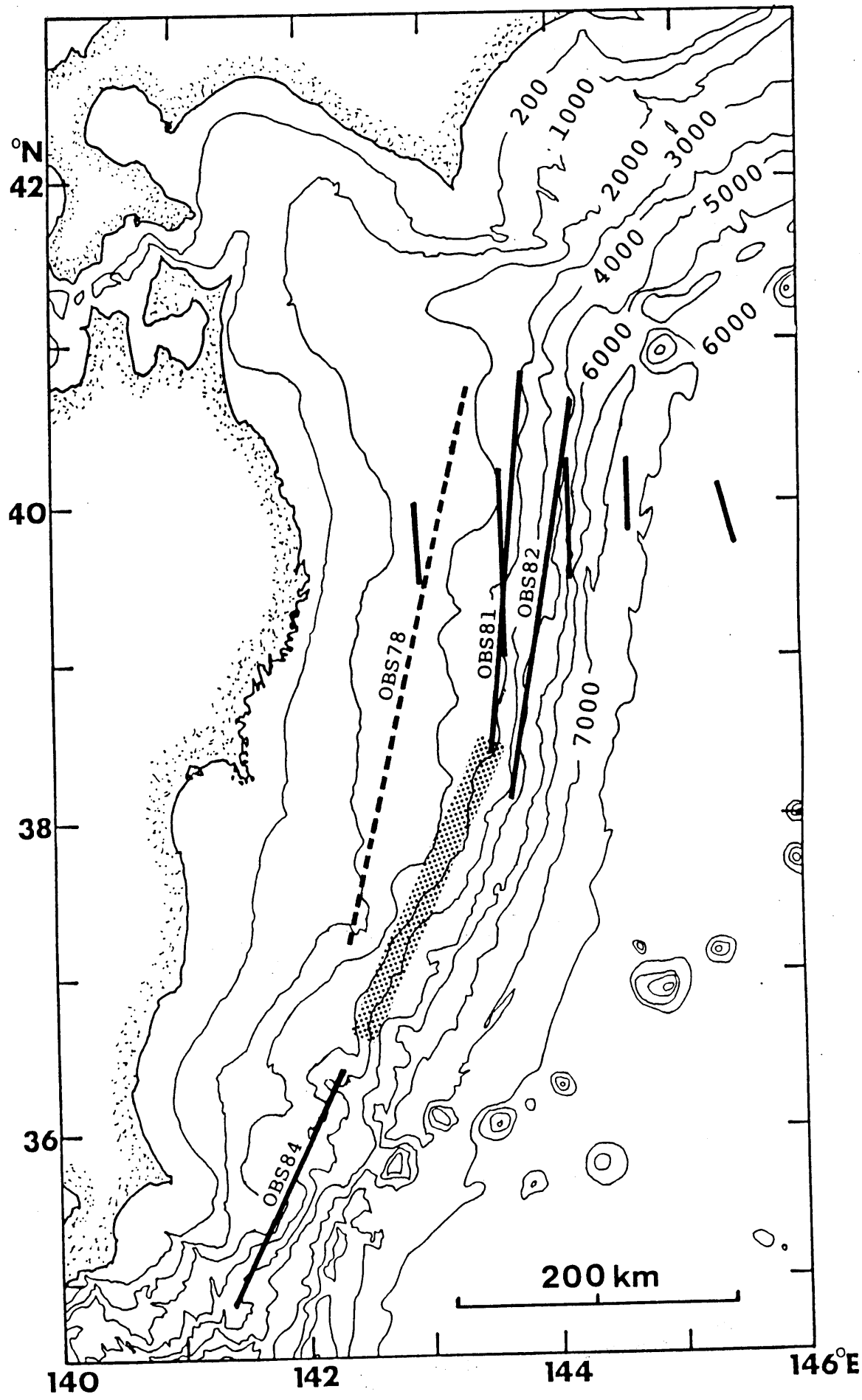
°N
42
40
38
36
140
142
144
146°E
200
1000
2000
3000
4000
5000
6000
6000
7000
OBS78
OBS81
OBS82
OBS84
200 km

FIG. 1.4

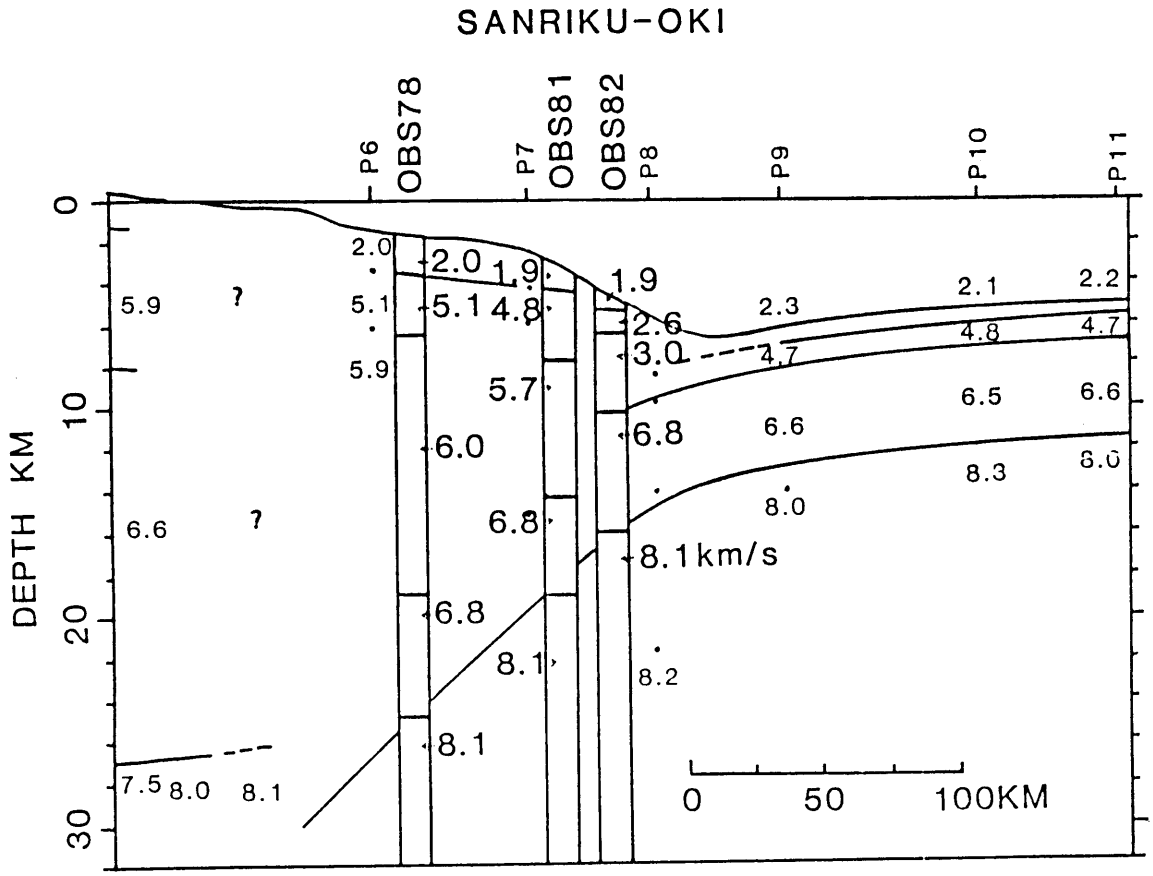
SANRIKU-OKI
P6
OBS78
P7
OBS81
OBS82
P8
P9
P10
P11
DEPTH KM
0
10
20
30
5.9
?
2.0
5.1
5.9
2.0
5.1
1.9
4.8
5.7
6.0
6.8
8.1
1.9
2.6
3.0
6.8
8.1km/s
8.2
2.3
4.7
6.6
8.0
2.1
4.8
6.5
8.3
2.2
4.7
6.6
8.0
6.6
?
6.8
8.1
7.5
8.0
8.1
0
50
100KM

FIG. 1.5

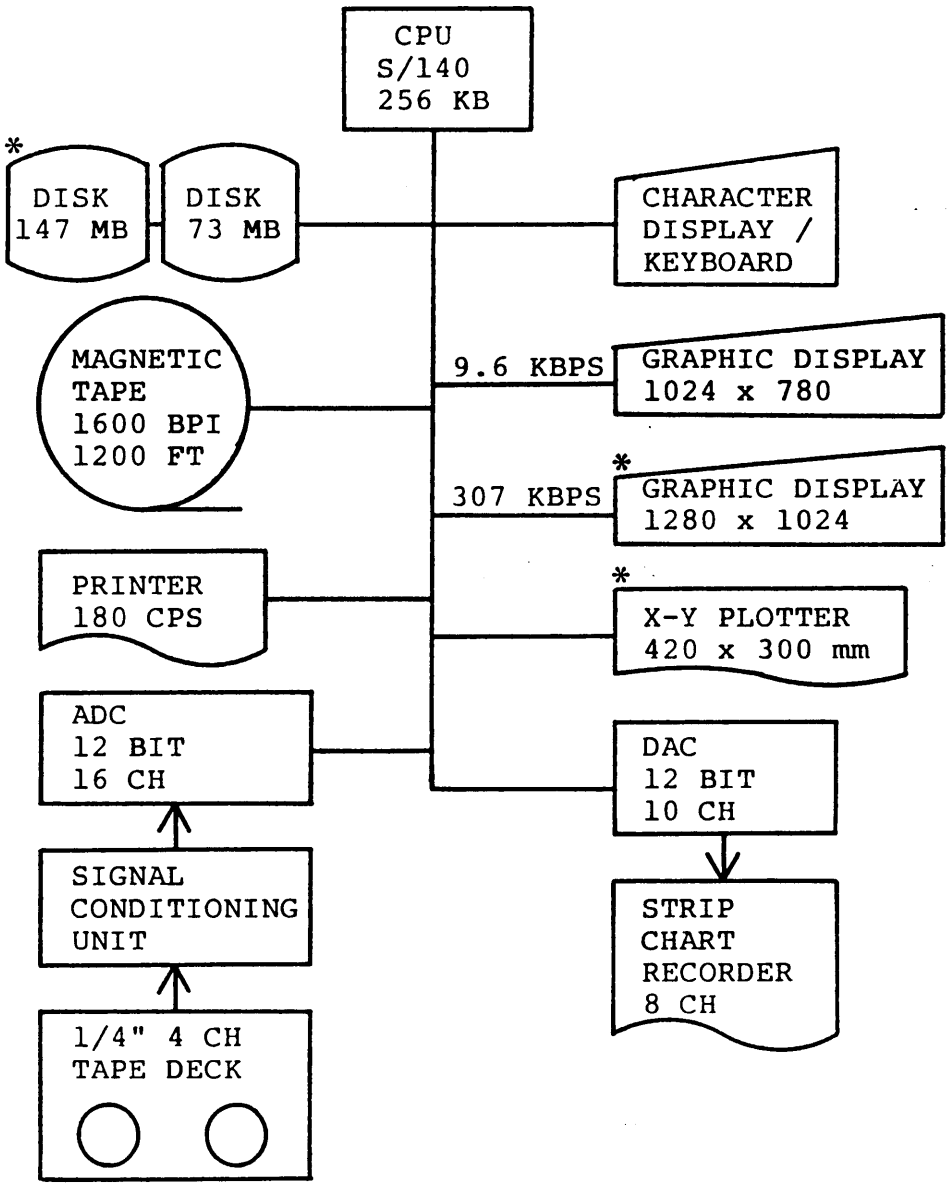
CPU
S/140
256 KB
*
DISK
147 MB
DISK
73 MB
CHARACTER
DISPLAY /
KEYBOARD
MAGNETIC
TAPE
1600 BPI
1200 FT
9.6 KBPS
GRAPHIC DISPLAY
1024 x 780
*
307 KBPS
GRAPHIC DISPLAY
1280 x 1024
PRINTER
180 CPS
*
X-Y PLOTTER
420 x 300 mm
ADC
12 BIT
16 CH
DAC
12 BIT
10 CH
SIGNAL
CONDITIONING
UNIT
STRIP
CHART
RECORDER
8 CH
1/4" 4 CH
TAPE DECK

FIG. 3.1

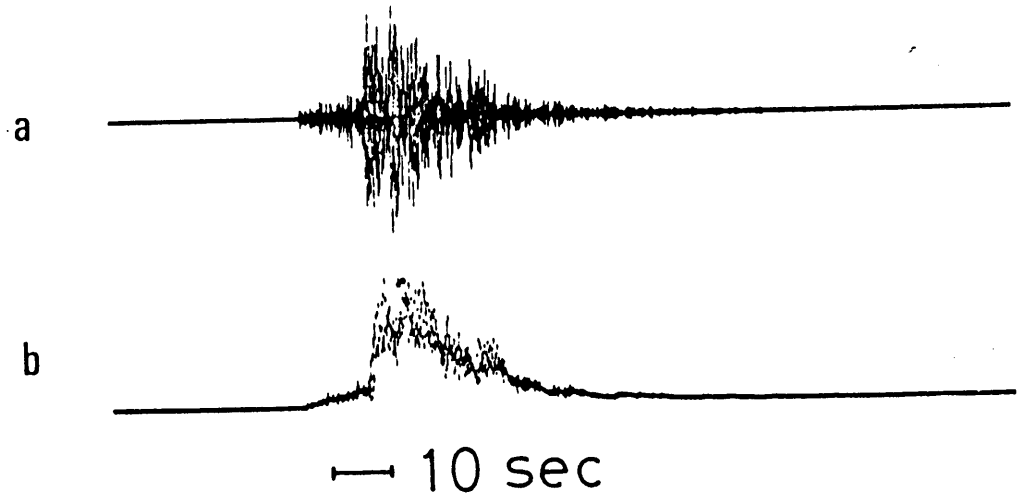


FIG. 3.2

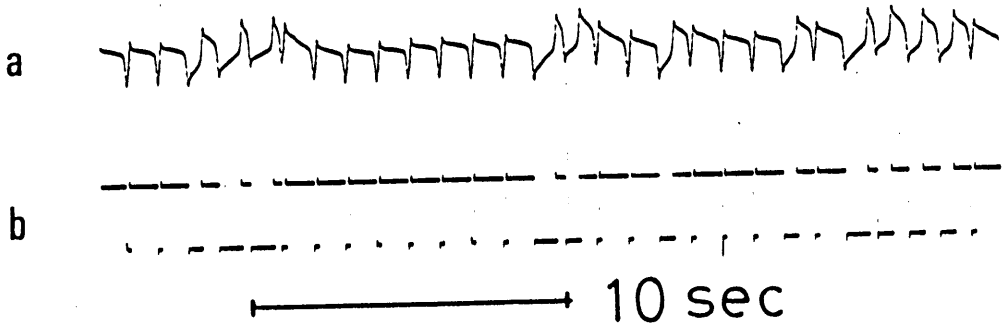


FIG. 3.3

(A)

| (1) | (2) | (3) | (4) | (5) | (6) | (7) | (8) | (9) | (10) |
|---|---|---|---|---|---|---|---|---|---|
| 10 | 16095510 | 26.8 | 43. | 782. | 822401 | 14.3 | 14.6 | 254 | 84 |
| 11 | 16100955 | 30.0 | 107. | 1178. | 822401 | 14.4 | 13.6 | 260 | 576 |
| 12 | 16101612 | 43.2 | 151. | 2011. | 822401 | 14.3 | 14.0 | 262 | 1907 |
| 13 | 16102036 | 104.1 | 1009. | 17021. | 822401 | 14.3 | 14.8 | 264 | 1624 |
| 14 | 16104901 | 84.6 | 96. | 2879. | 822401 | 14.3 | 16.2 | 276 | 1657 |

(B)

| (1) | (2) | (3) |
|---|---|---|
| 19024553 | 195 | 1 |
| 19032305 | 108 | 3 |
| 19032835 | 155 | 1 |
| 19041404 | 90 | 3 |
| 19045441 | 113 | 3 |

(C)

| (1) | (2) | (3) | (4) | (5) | (6) | (7) | (8) | (9) | (10) |
|---|---|---|---|---|---|---|---|---|---|
| 1 | 38001635000 | 105.57 | 2441 | 0 | 9 | 4096 | 8201 | -1 | -4 |
| 2 | 38015615000 | 105.59 | 2441 | 9 | 9 | 4096 | 8201 | -1 | -3 |
| 3 | 38042443000 | 105.65 | 1221 | 18 | 9 | 4096 | 8201 | -1 | -3 |
| 4 | 38055309000 | 105.64 | 2441 | 27 | 9 | 4096 | 8201 | -1 | -1 |
| 5 | 38061615000 | 105.63 | 2441 | 36 | 9 | 4096 | 8201 | -1 | -2 |

FIG. 3.4

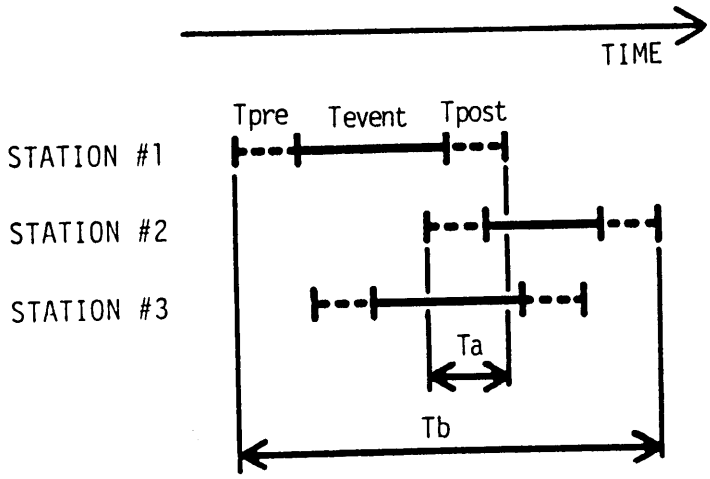


FIG. 3.5

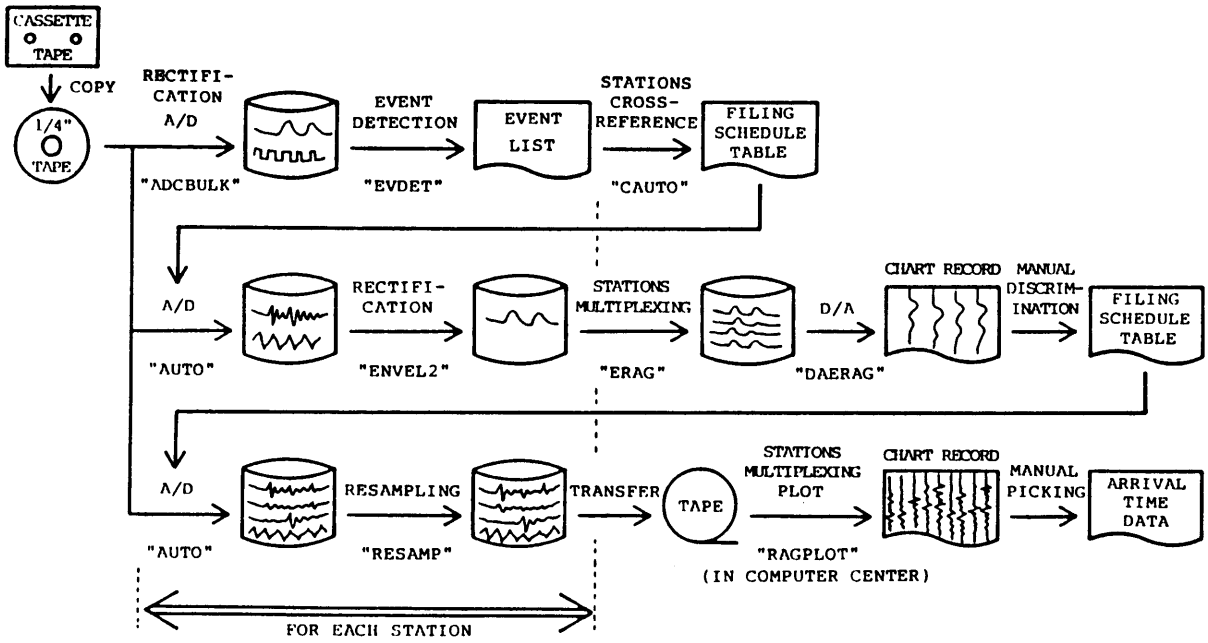
CASSETTE TAPE
COPY
1/4" TAPE
RECTIFI-CATION A/D
"ADCBULK"
EVENT DETECTION
"EVDET"
EVENT LIST
STATIONS CROSS-REFERENCE
"CAUTO"
FILING SCHEDULE TABLE
A/D
"AUTO"
RECTIFI-CATION
"ENVEL2"
STATIONS MULTIPLEXING
"ERAG"
D/A
"DAERAG"
CHART RECORD
MANUAL DISCRIM-INATION
FILING SCHEDULE TABLE
A/D
"AUTO"
RESAMPLING
"RESAMP"
TRANSFER
TAPE
STATIONS MULTIPLEXING PLOT
"RAGPLOT"
(IN COMPUTER CENTER)
CHART RECORD
MANUAL PICKING
ARRIVAL TIME DATA
FOR EACH STATION

FIG. 3.6

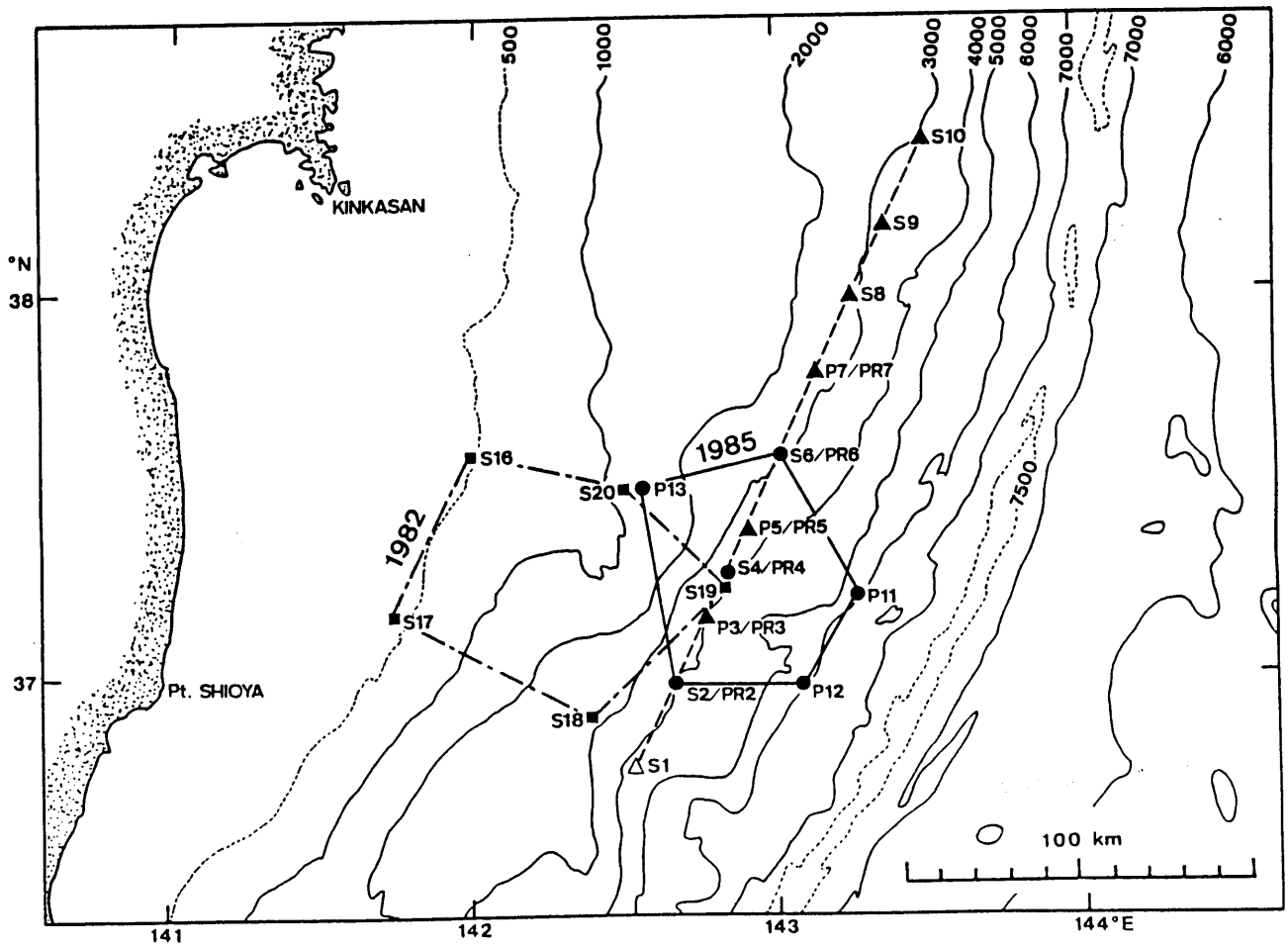
KINKASAN
Pt. SHIOYA
°N
38
37
141
142
143
144°E
500
1000
2000
3000
4000
5000
6000
7000
7000
6000
7500
S10
S9
S8
P7/PR7
S6/PR6
P5/PR5
S4/PR4
P11
P3/PR3
P12
S2/PR2
S1
P13
S20
S16
S17
S18
S19
1985
1982
100 km

FIG. 4.1

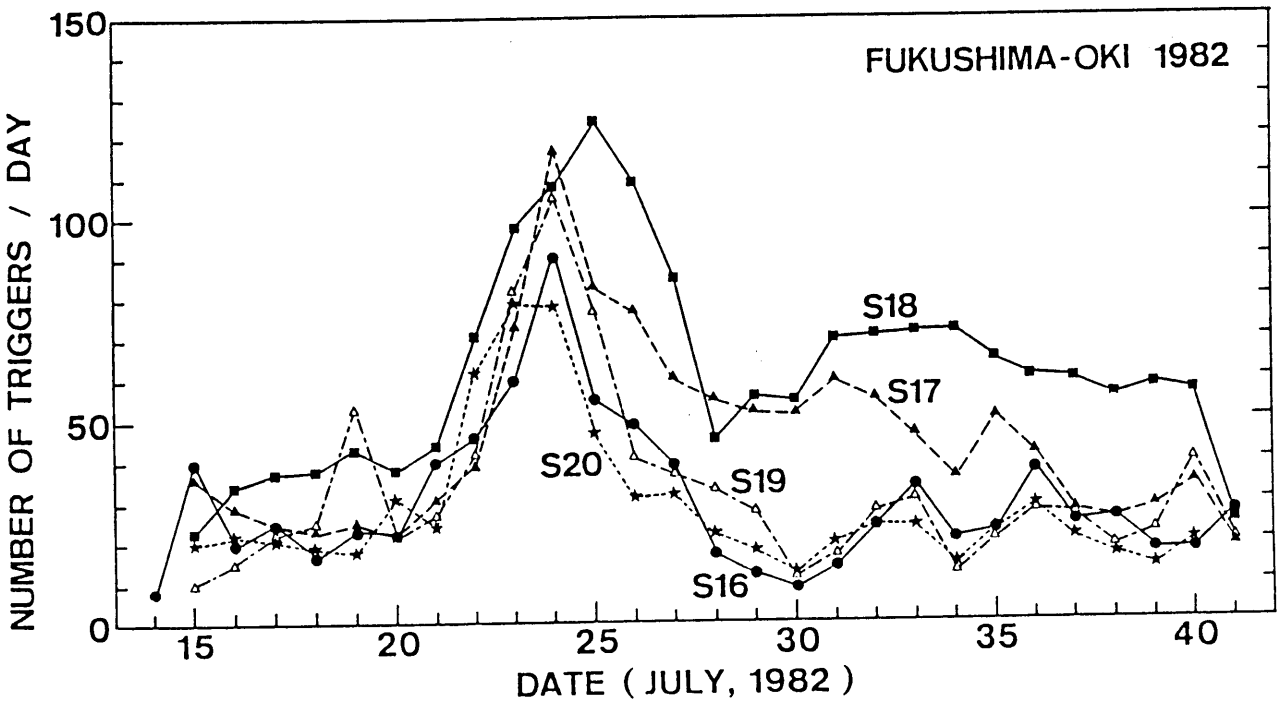
FUKUSHIMA-OKI 1982
NUMBER OF TRIGGERS / DAY
DATE ( JULY, 1982 )
150
100
50
0
15
20
25
30
35
40
S18
S17
S20
S19
S16

FIG. 4.2

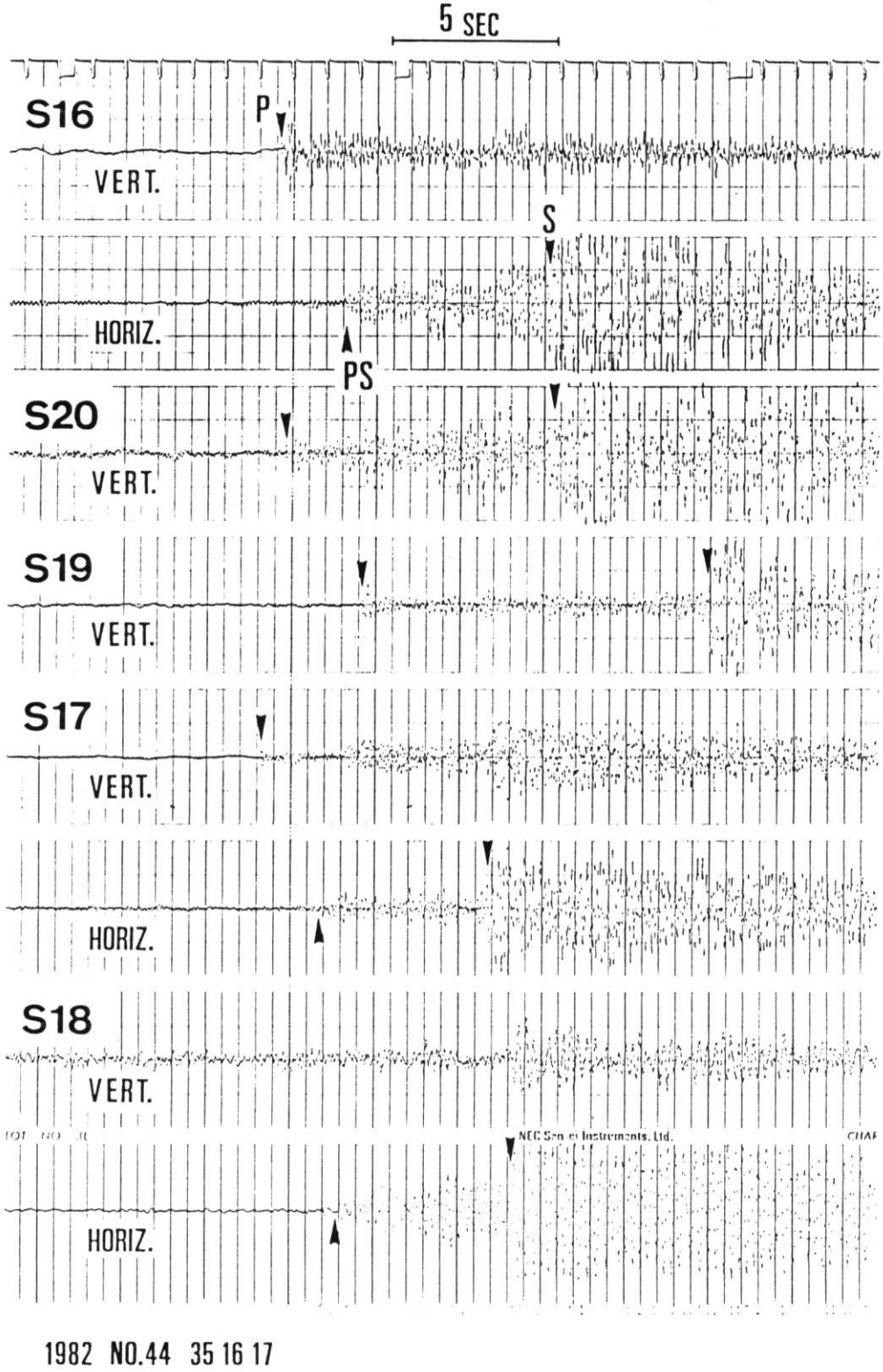
5 SEC
S16
P
VERT.
S
HORIZ.
PS
S20
VERT.
S19
VERT.
S17
VERT.
HORIZ.
S18
VERT.
HORIZ.
1982 NO.44 35 16 17

FIG. 4.3

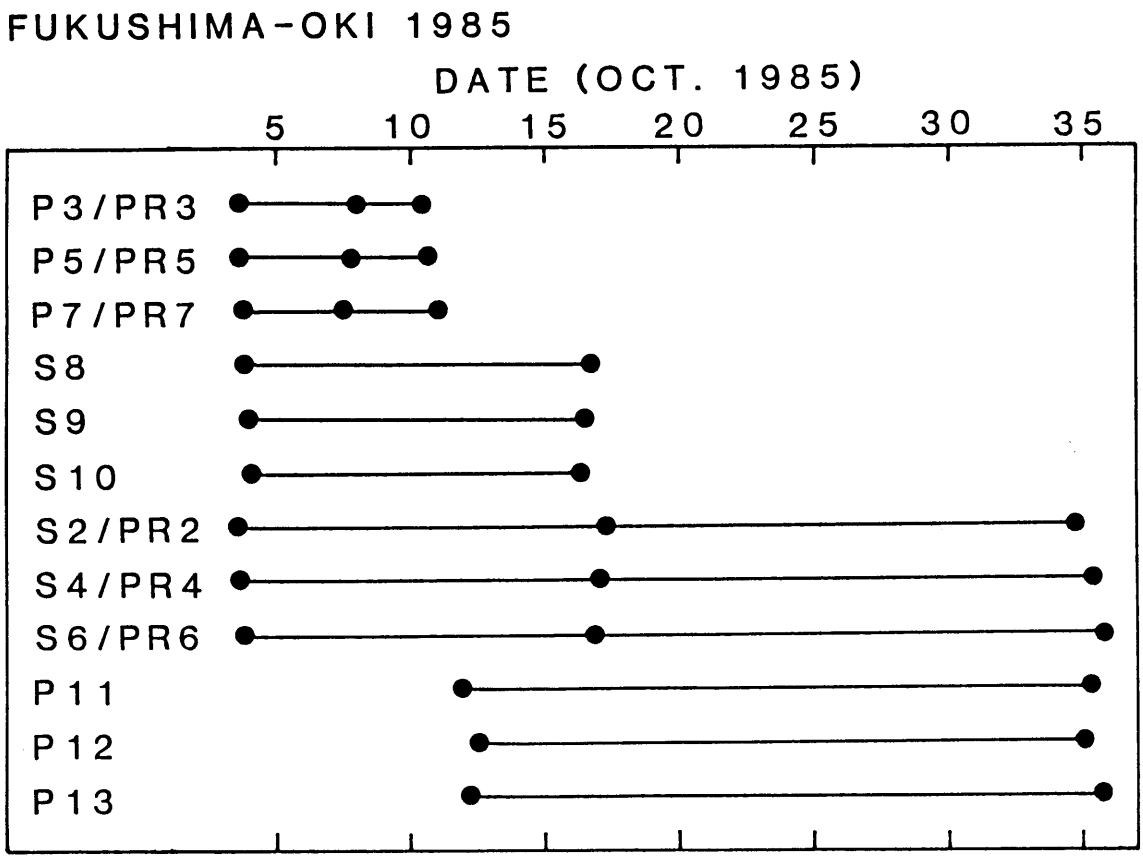
FUKUSHIMA-OKI 1985
DATE (OCT. 1985)
5
10
15
20
25
30
35
P3/PR3
P5/PR5
P7/PR7
S8
S9
S10
S2/PR2
S4/PR4
S6/PR6
P11
P12
P13

FIG. 4.4

S2

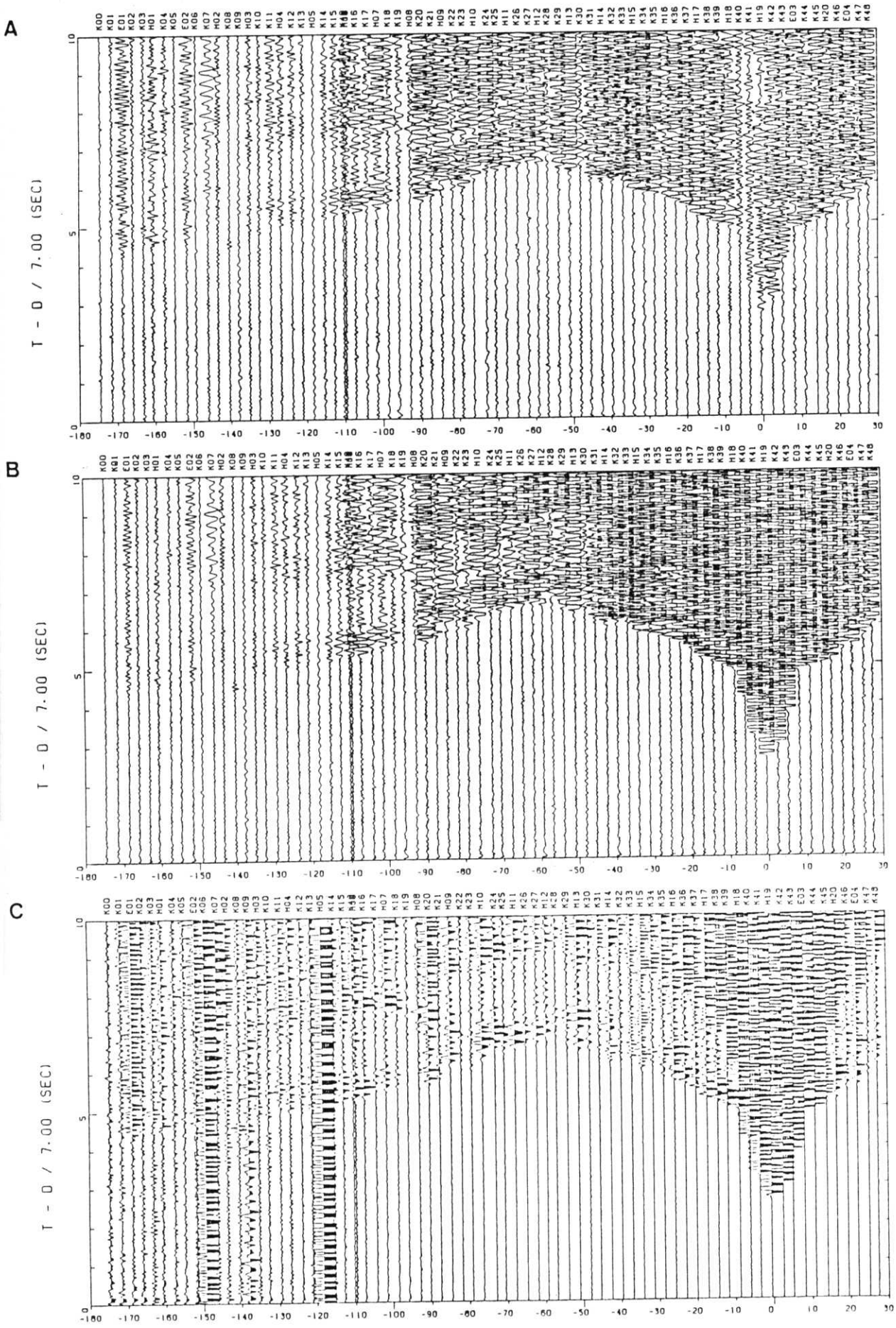


FIG. 4.5

P3/PR3

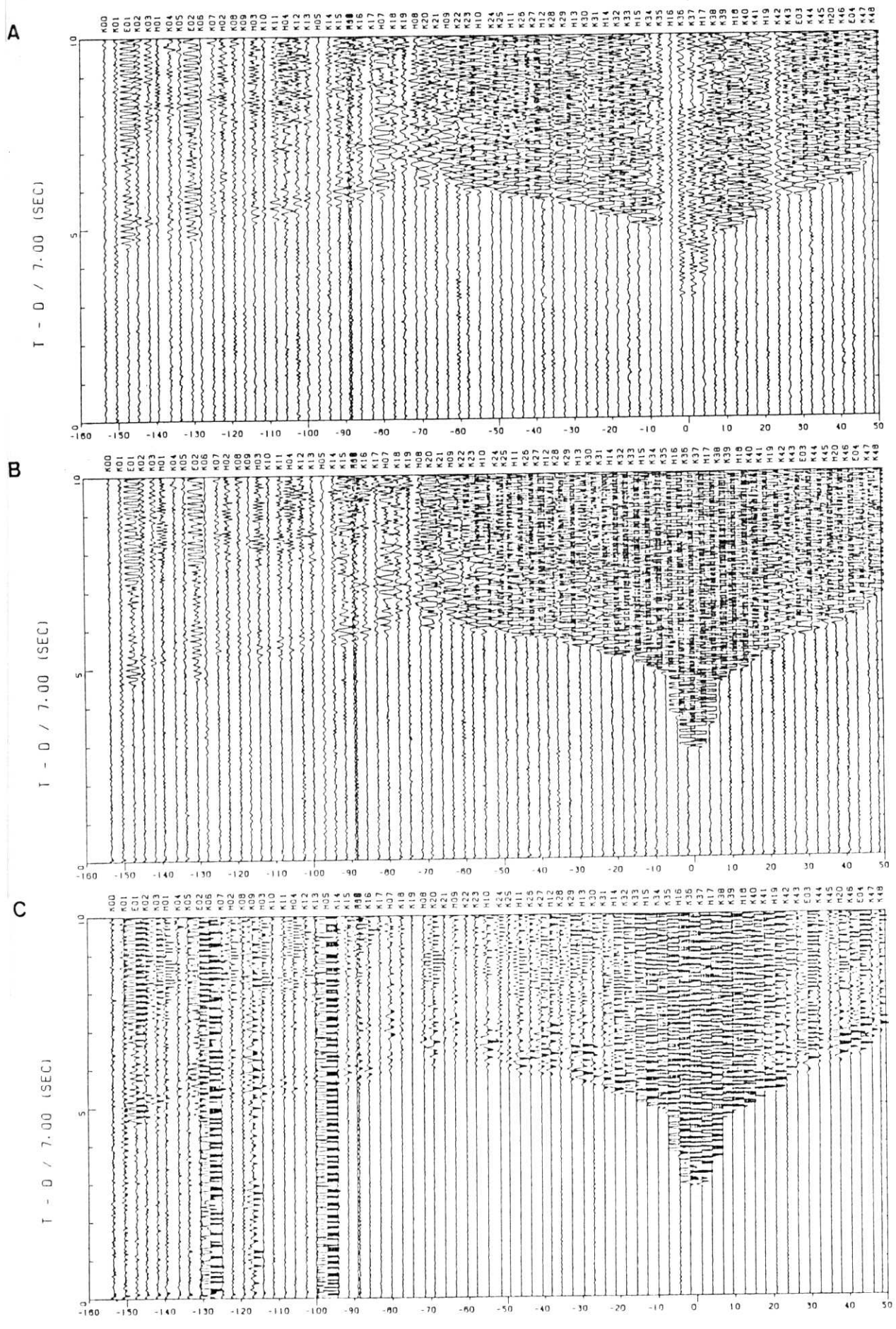


FIG. 4.6

S4

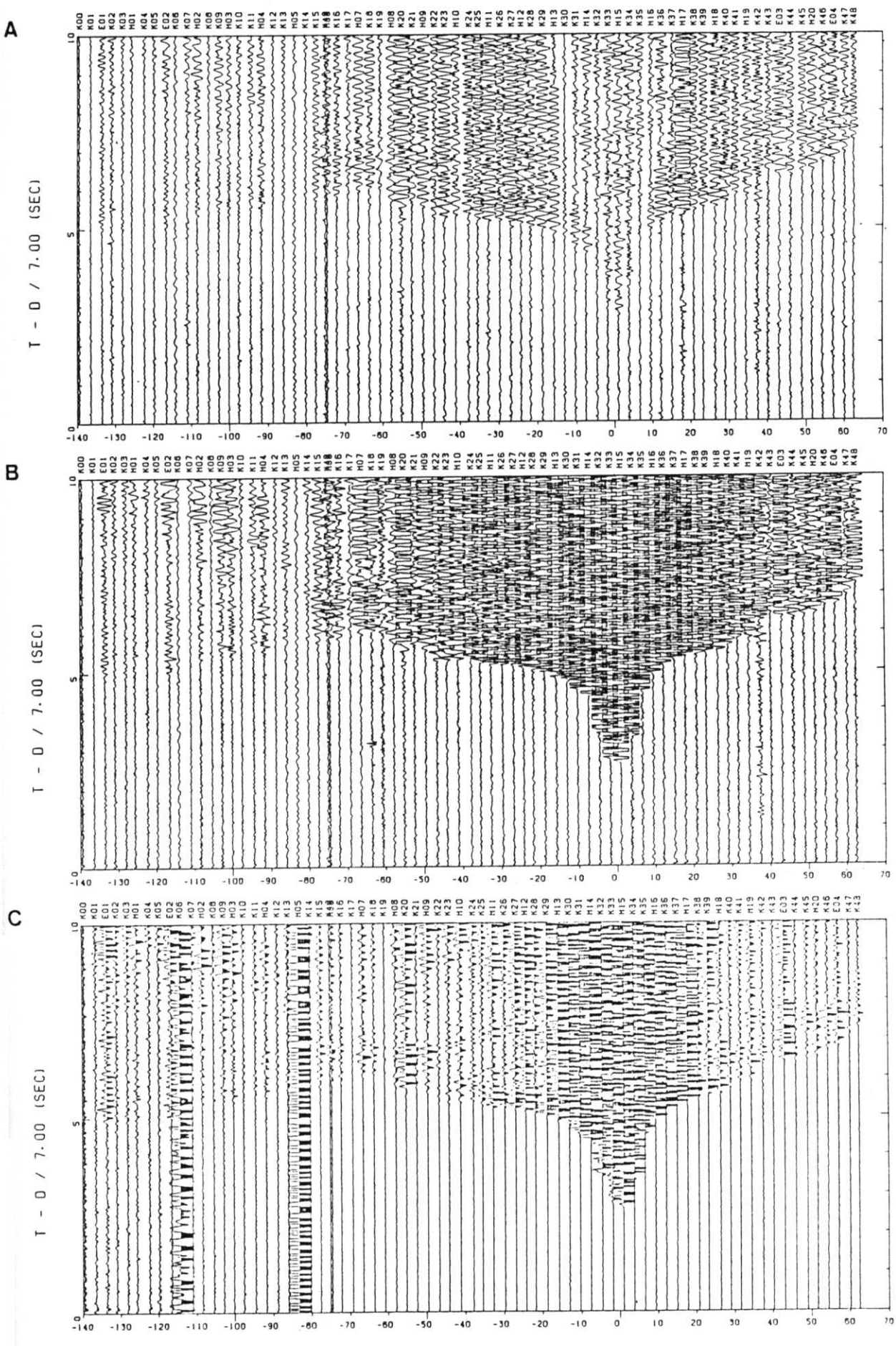


FIG. 4.7

P5/PR5

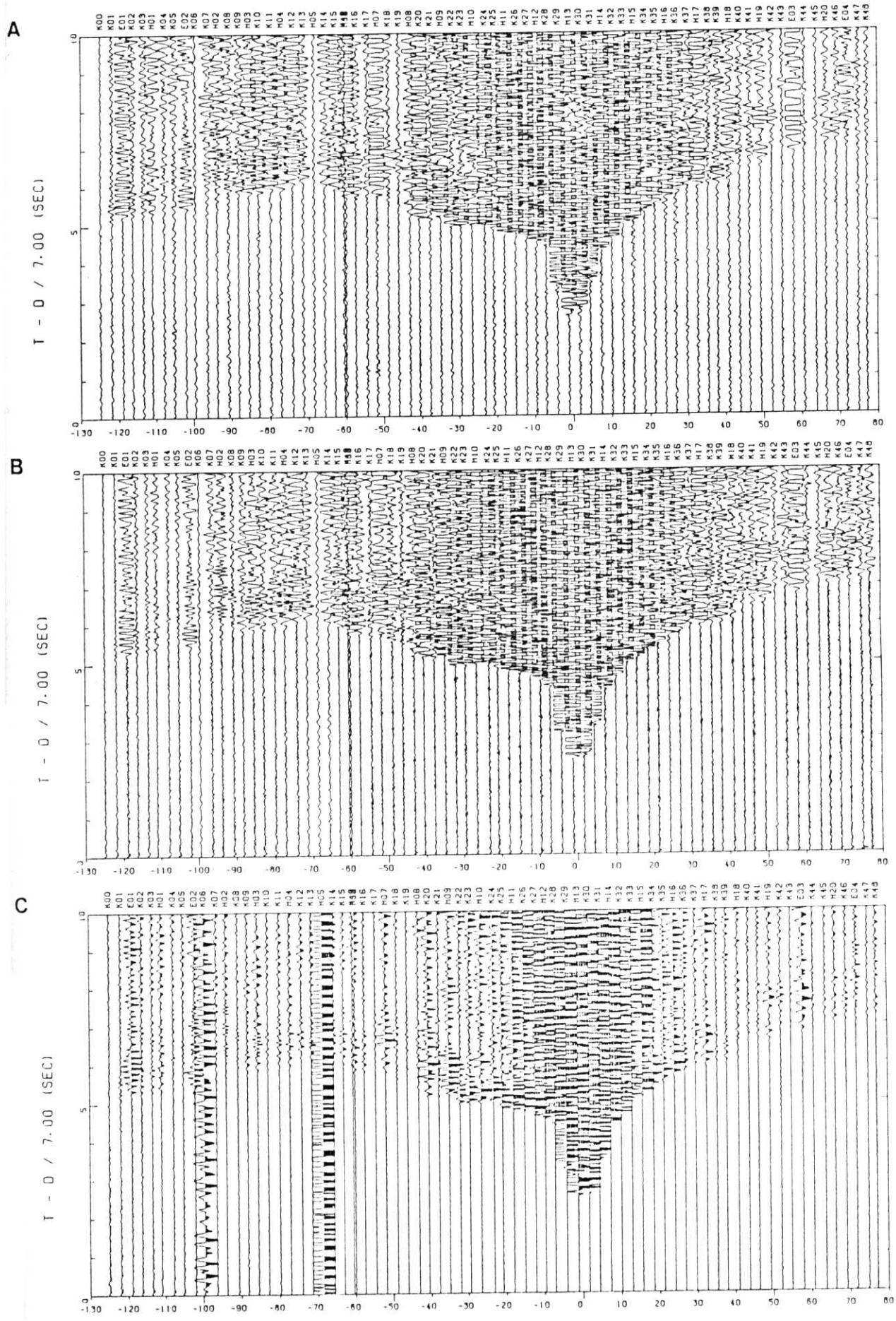


FIG. 4.8

S6

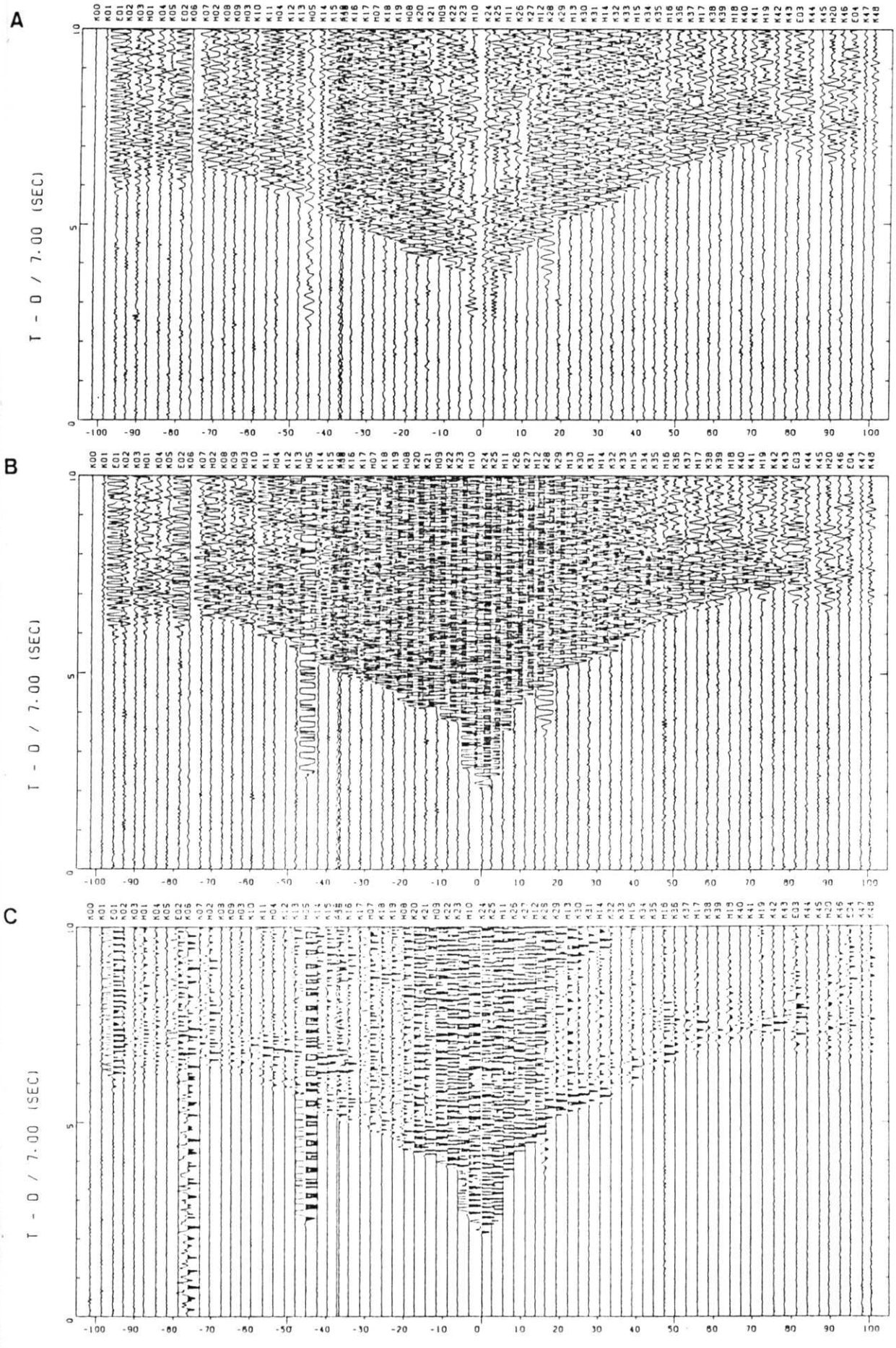


FIG. 4.9

P7/PR7

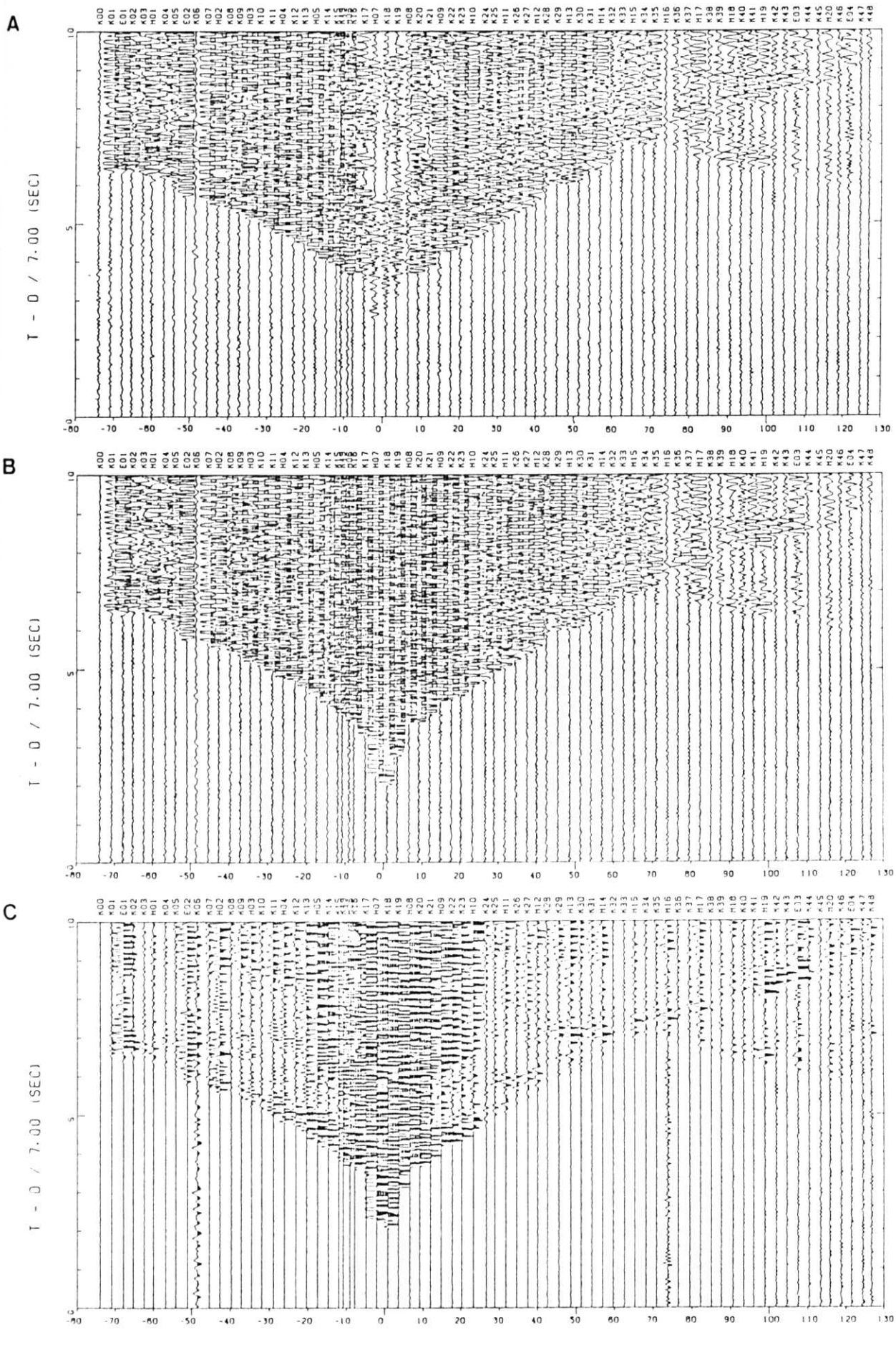


FIG. 4.10

S9

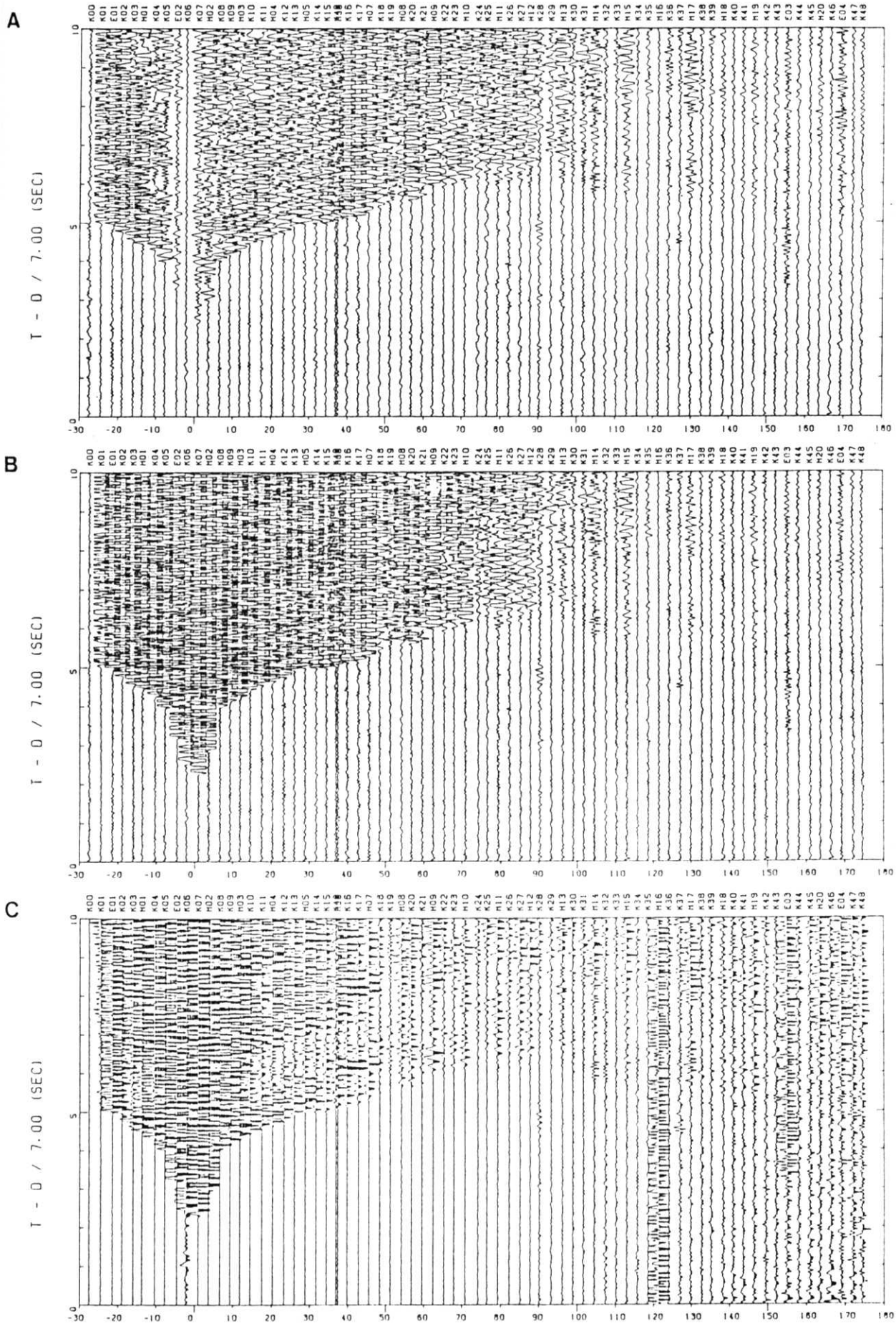


FIG. 4.11

S10

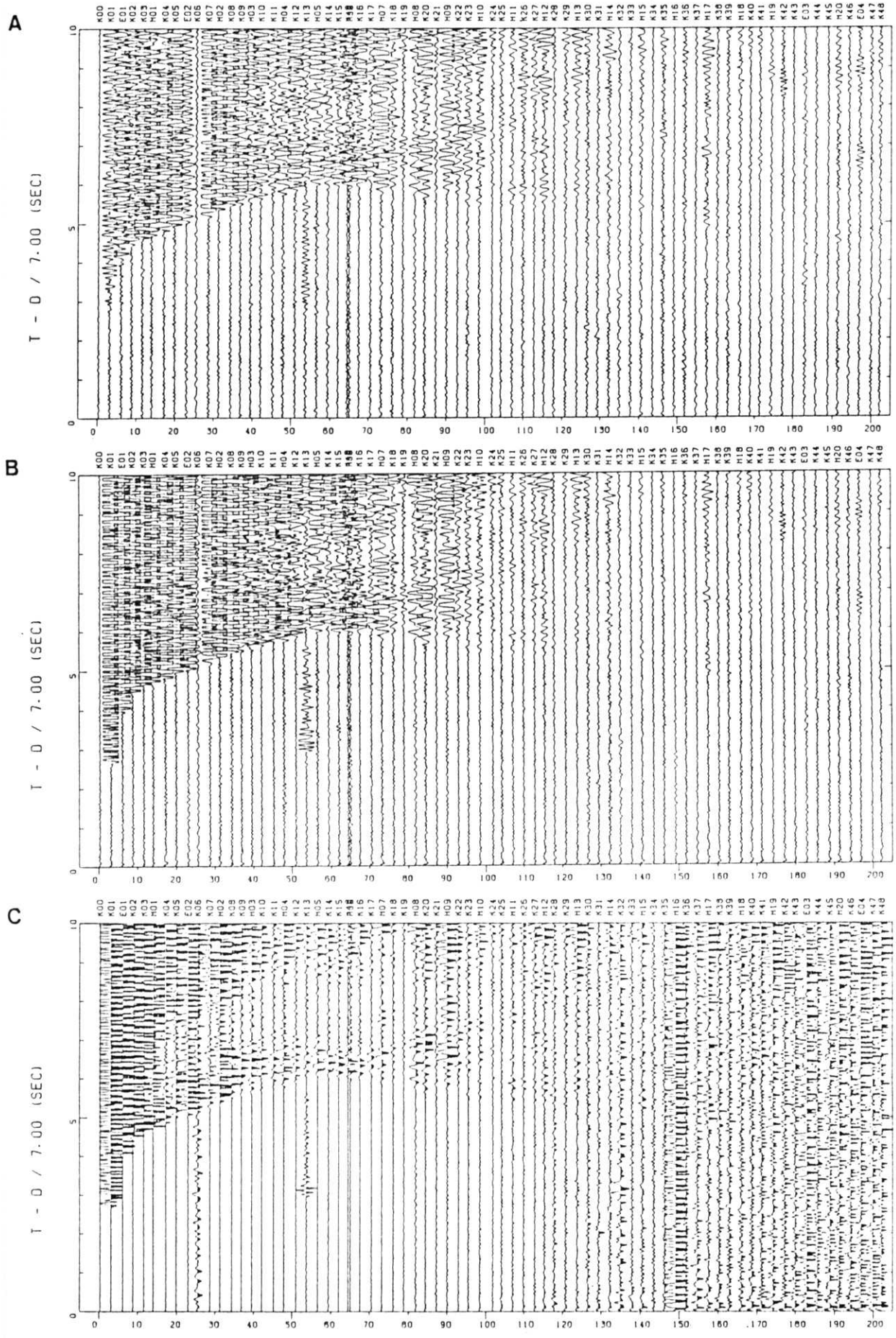


FIG. 4.12

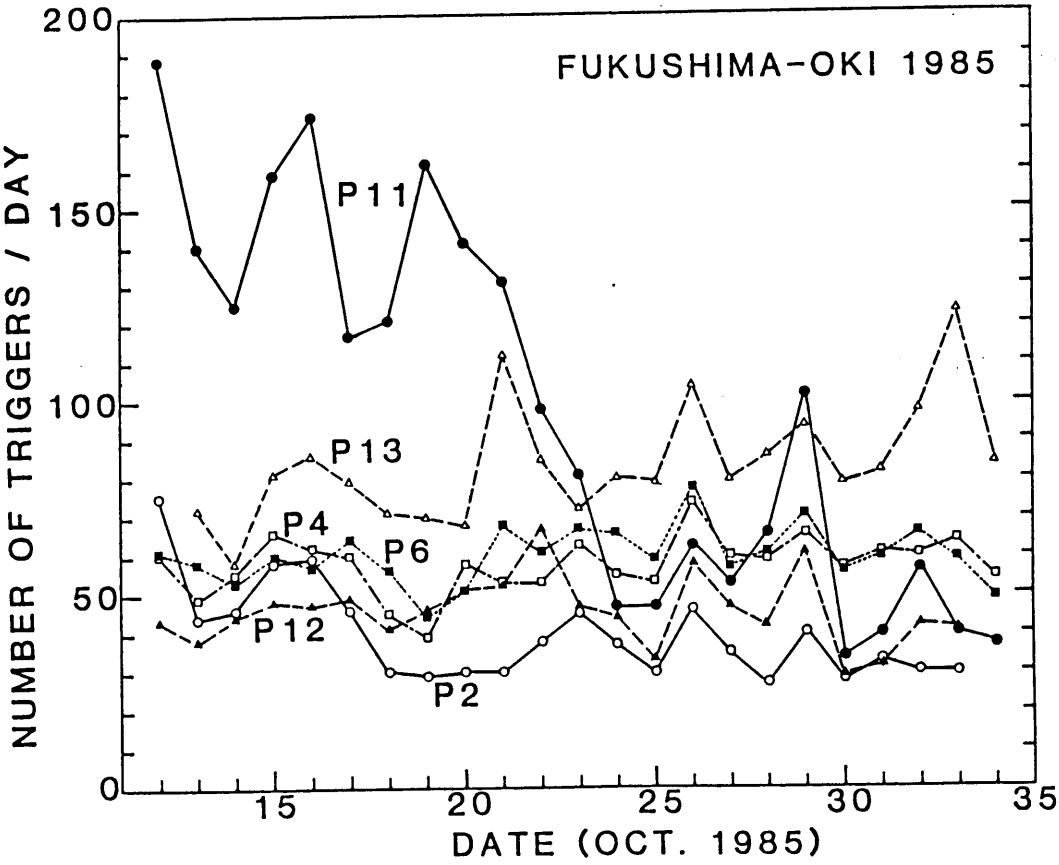
FUKUSHIMA-OKI 1985
NUMBER OF TRIGGERS / DAY
DATE (OCT. 1985)
P11
P13
P4
P6
P12
P2
200
150
100
50
0
15
20
25
30
35

FIG. 4.13

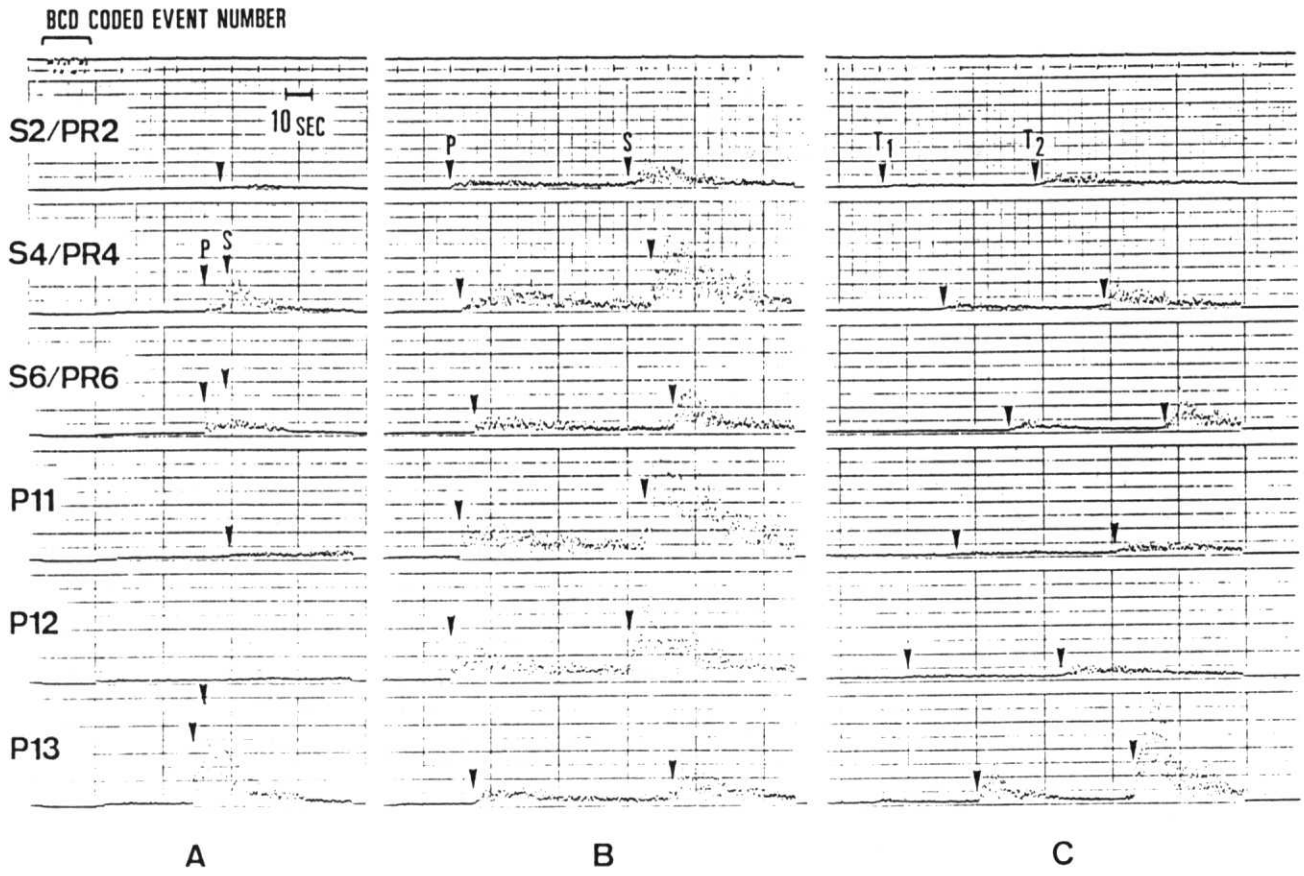
BCD CODED EVENT NUMBER
S2/PR2
10 SEC
S4/PR4
P
S
S6/PR6
P11
P12
P13
P
S
T1
T2
A
B
C

FIG. 4.14

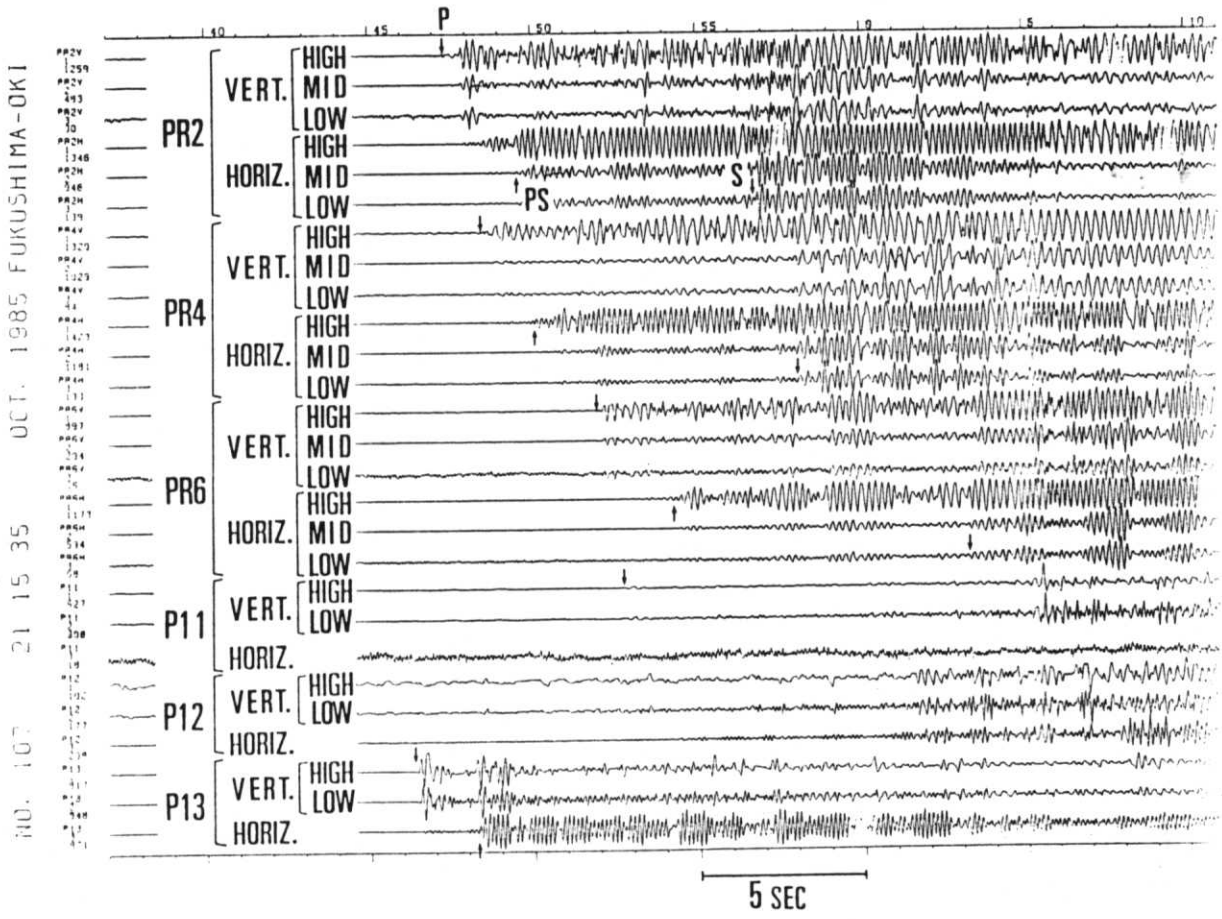
NO. 107 21 15 35 OCT. 1985 FUKUSHIMA-OKI
P
S
PS
PR2
PR4
PR6
P11
P12
P13
VERT.
HORIZ.
HIGH
MID
LOW
5 SEC

FIG. 4.15

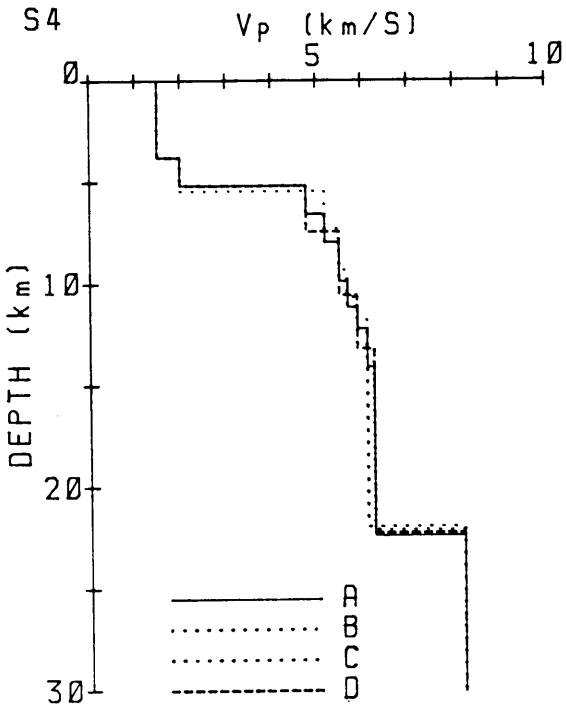


FIG. 5.1

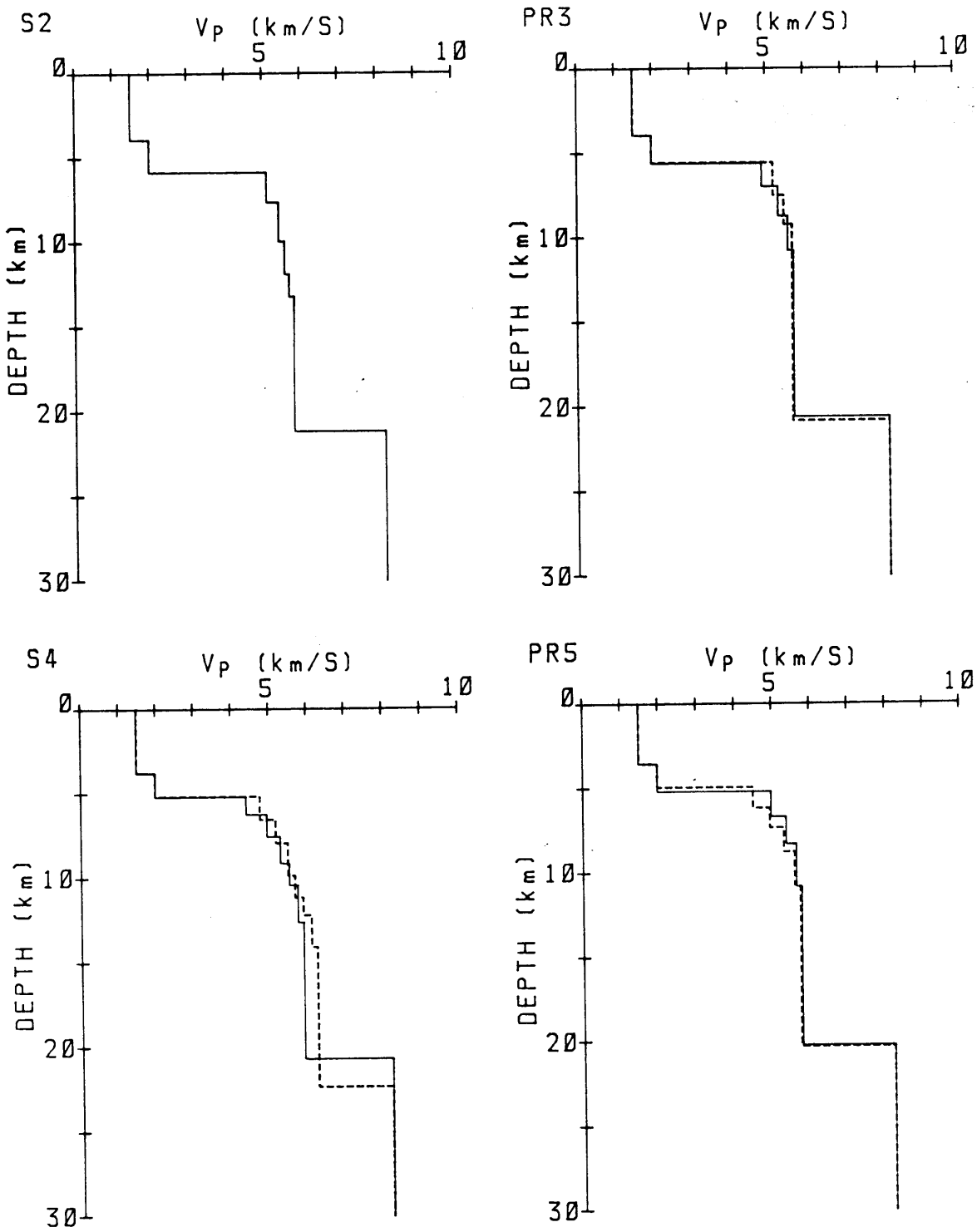
S2
Vp (km/S)
0
5
10
DEPTH (km)
10
20
30
PR3
Vp (km/S)
0
5
10
DEPTH (km)
10
20
30
S4
Vp (km/S)
0
5
10
DEPTH (km)
10
20
30
PR5
Vp (km/S)
0
5
10
DEPTH (km)
10
20
30

FIG. 5.2

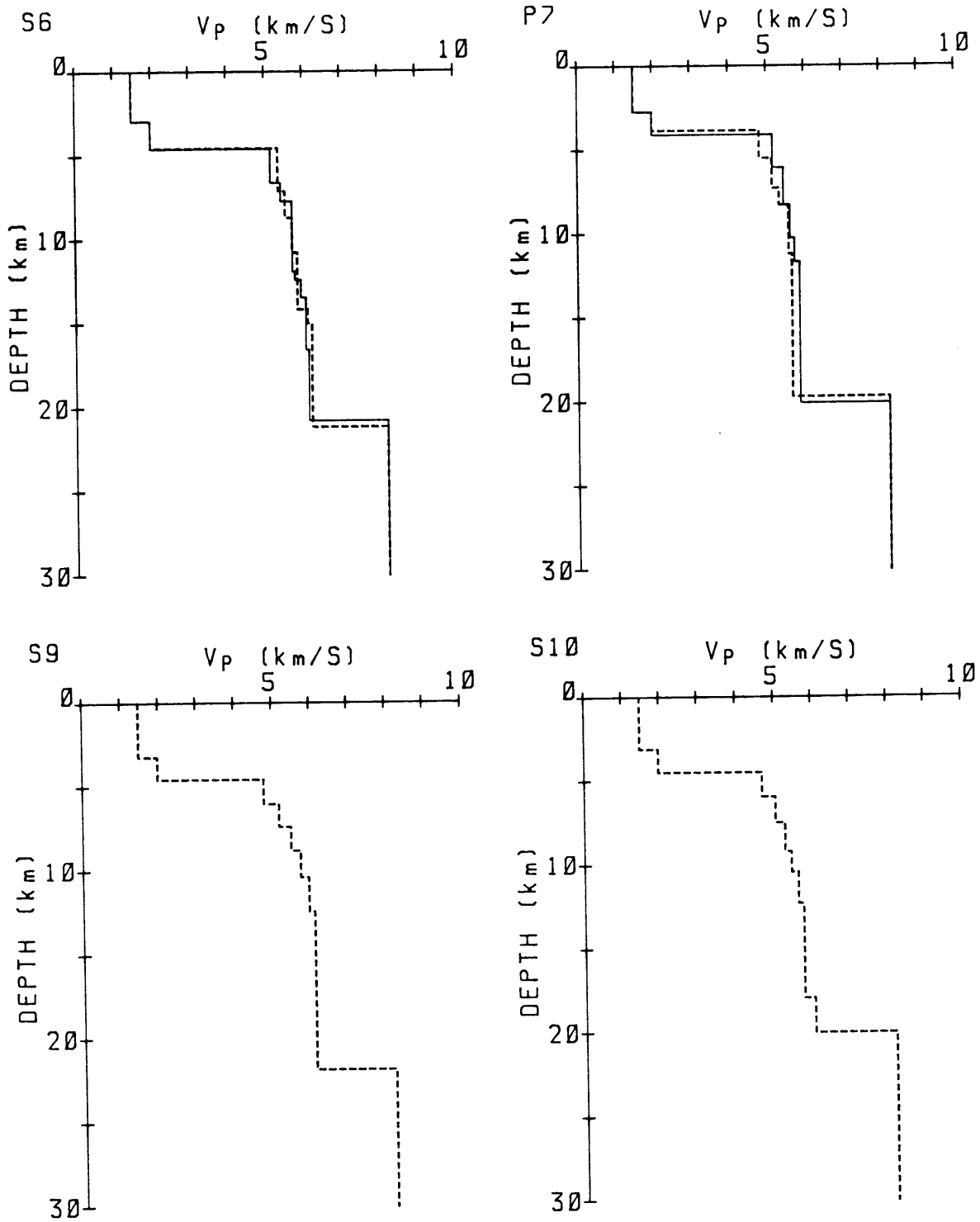


FIG. 5.2 (continued)

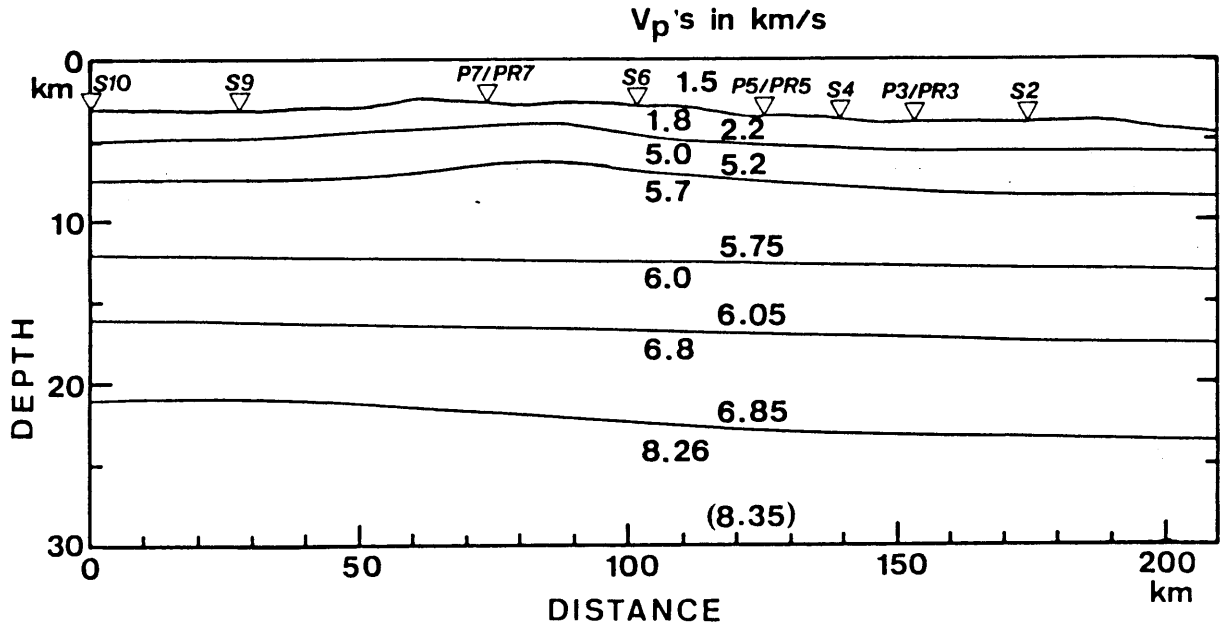
Vp's in km/s
0
km
S10
S9
P7/PR7
S6
1.5
P5/PR5
S4
P3/PR3
S2
1.8
2.2
5.0
5.2
5.7
10
5.75
6.0
6.05
6.8
20
6.85
8.26
(8.35)
30
0
50
100
150
200
km
DEPTH
DISTANCE

FIG. 5.3

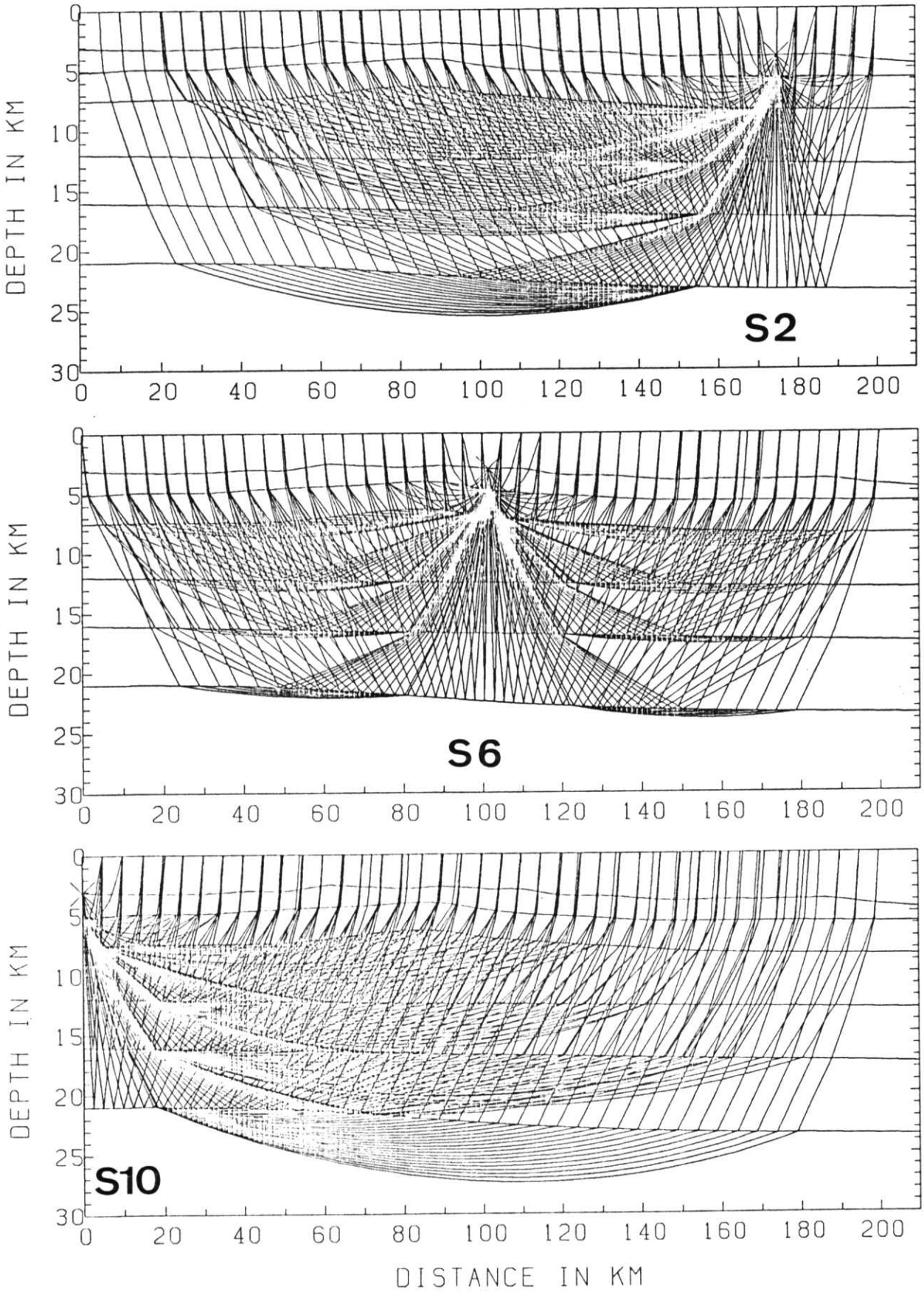
DEPTH IN KM
0
5
10
15
20
25
30
S2
0
20
40
60
80
100
120
140
160
180
200
DEPTH IN KM
S6
DEPTH IN KM
S10
DISTANCE IN KM

FIG. 5.4

# S2

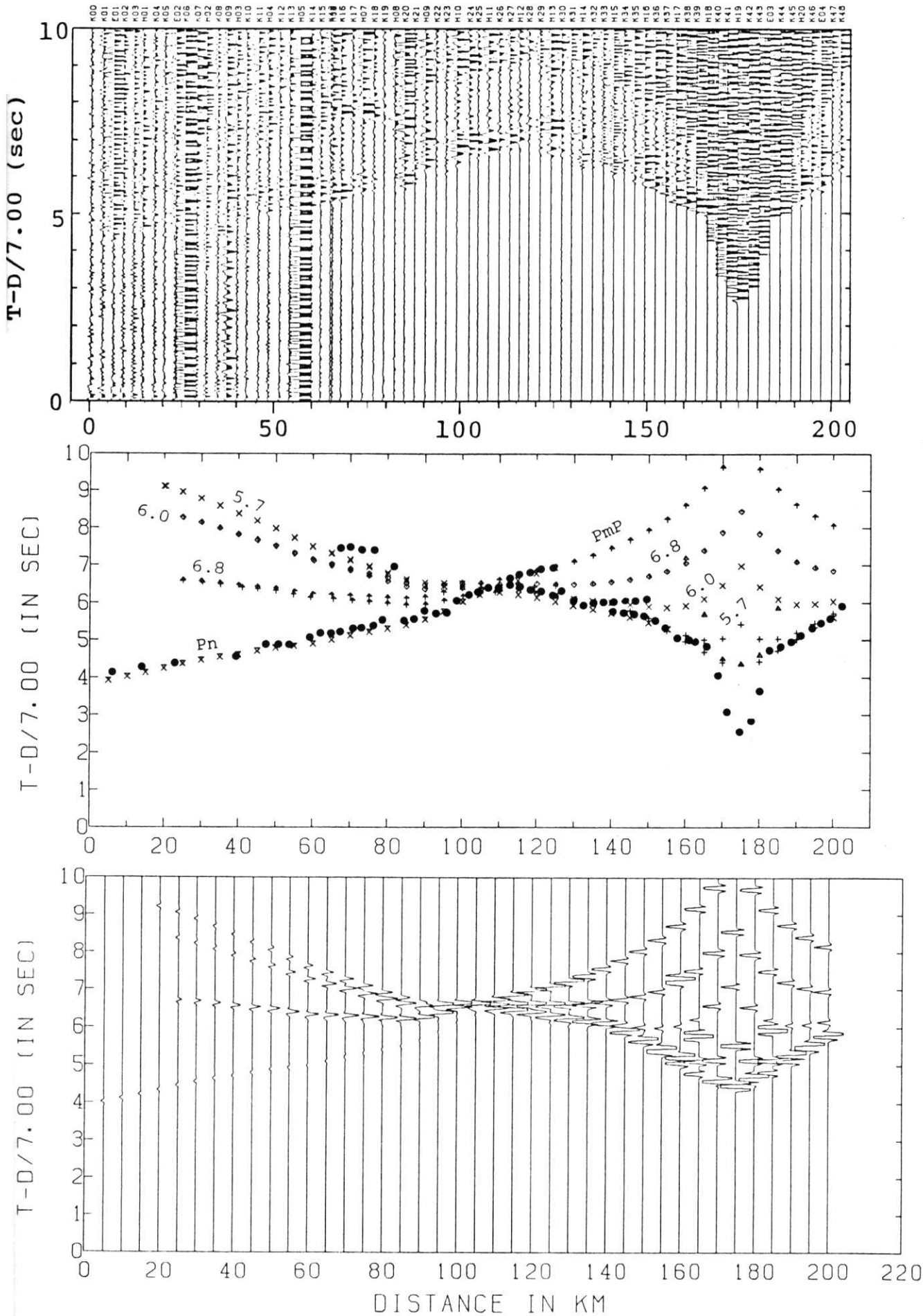
T-D/7.00 (sec)
T-D/7.00 (IN SEC)
T-D/7.00 (IN SEC)
6.0
5.7
6.8
Pn
PmP
6.8
6.0
5.7
DISTANCE IN KM

FIG. 5.5

# *P3/PR3*

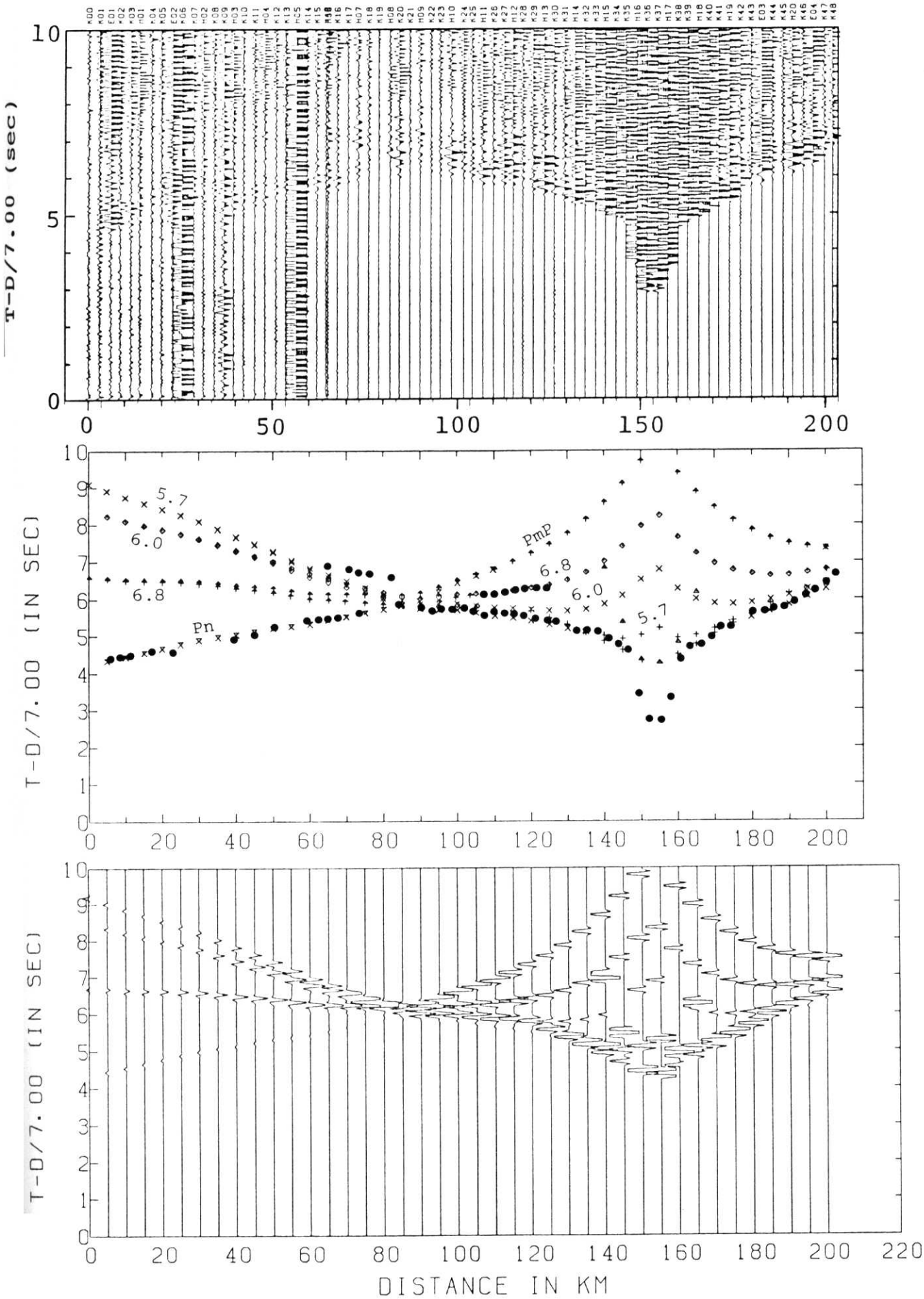
T-D/7.00 (sec)
10
5
0
0
50
100
150
200
T-D/7.00 (IN SEC)
5.7
6.0
6.8
Pn
PmP
6.8
6.0
5.7
0
20
40
60
80
100
120
140
160
180
200
T-D/7.00 (IN SEC)
DISTANCE IN KM
220

FIG. 5.6

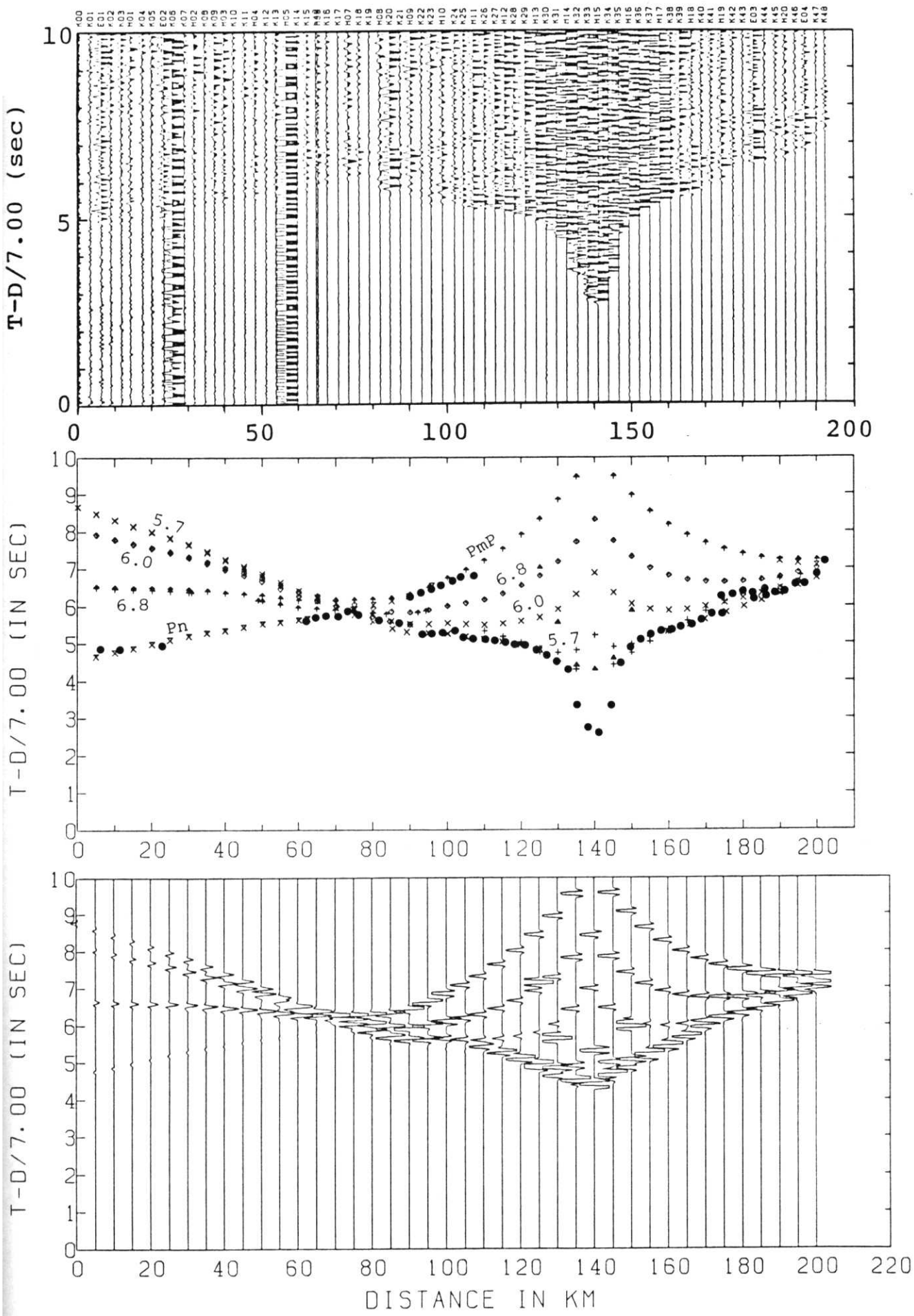
S4
T-D/7.00 (sec)
T-D/7.00 (IN SEC)
T-D/7.00 (IN SEC)
5.7
6.0
6.8
Pn
PmP
6.8
6.0
5.7
DISTANCE IN KM

FIG. 5.7

# *P5/PR5*

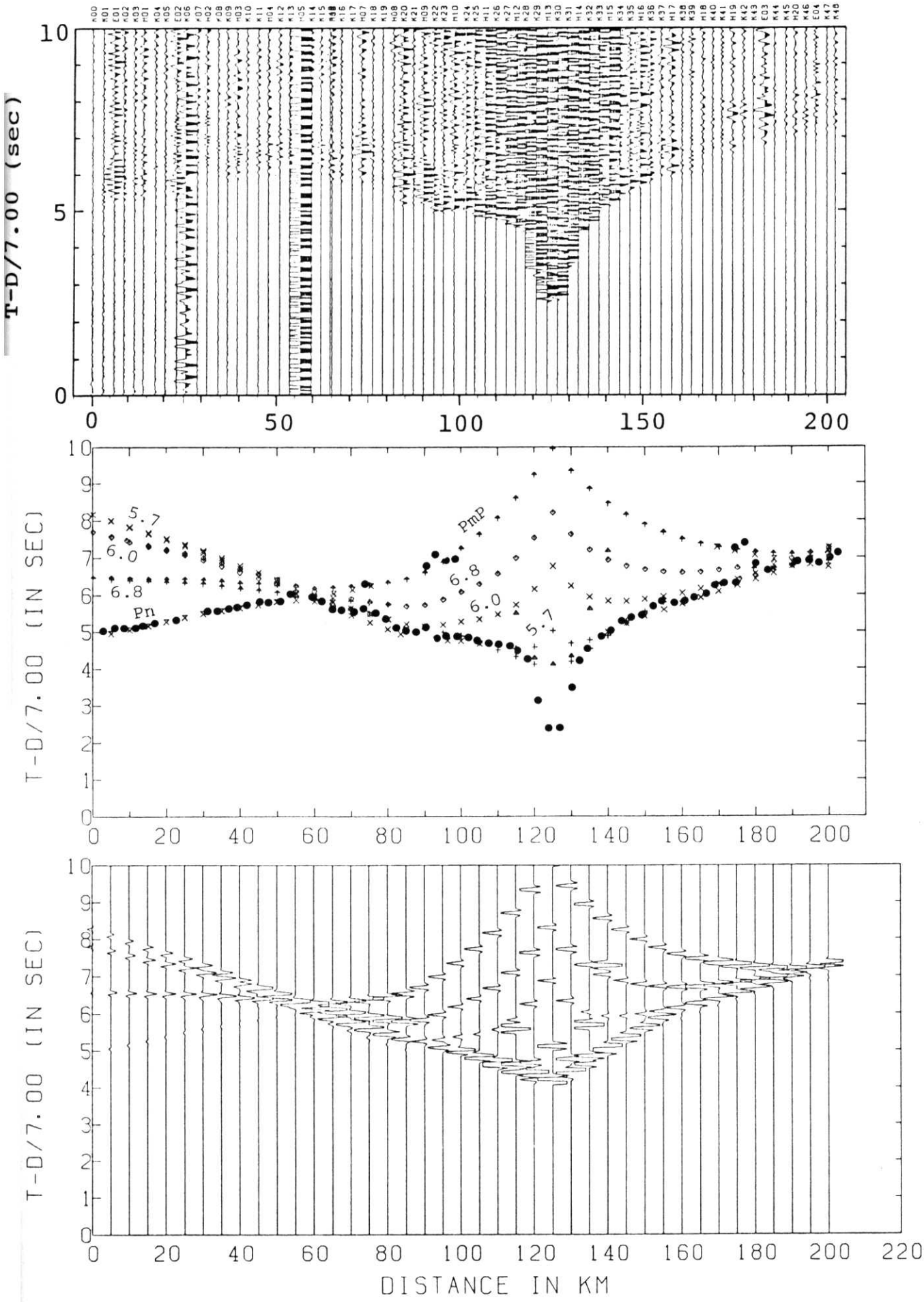
T-D/7.00 (sec)
10
5
0
0
50
100
150
200
T-D/7.00 (IN SEC)
5.7
6.0
6.8
Pn
PmP
6.8
6.0
5.7
0
20
40
60
80
100
120
140
160
180
200
T-D/7.00 (IN SEC)
DISTANCE IN KM
220

FIG. 5.8

*S6*

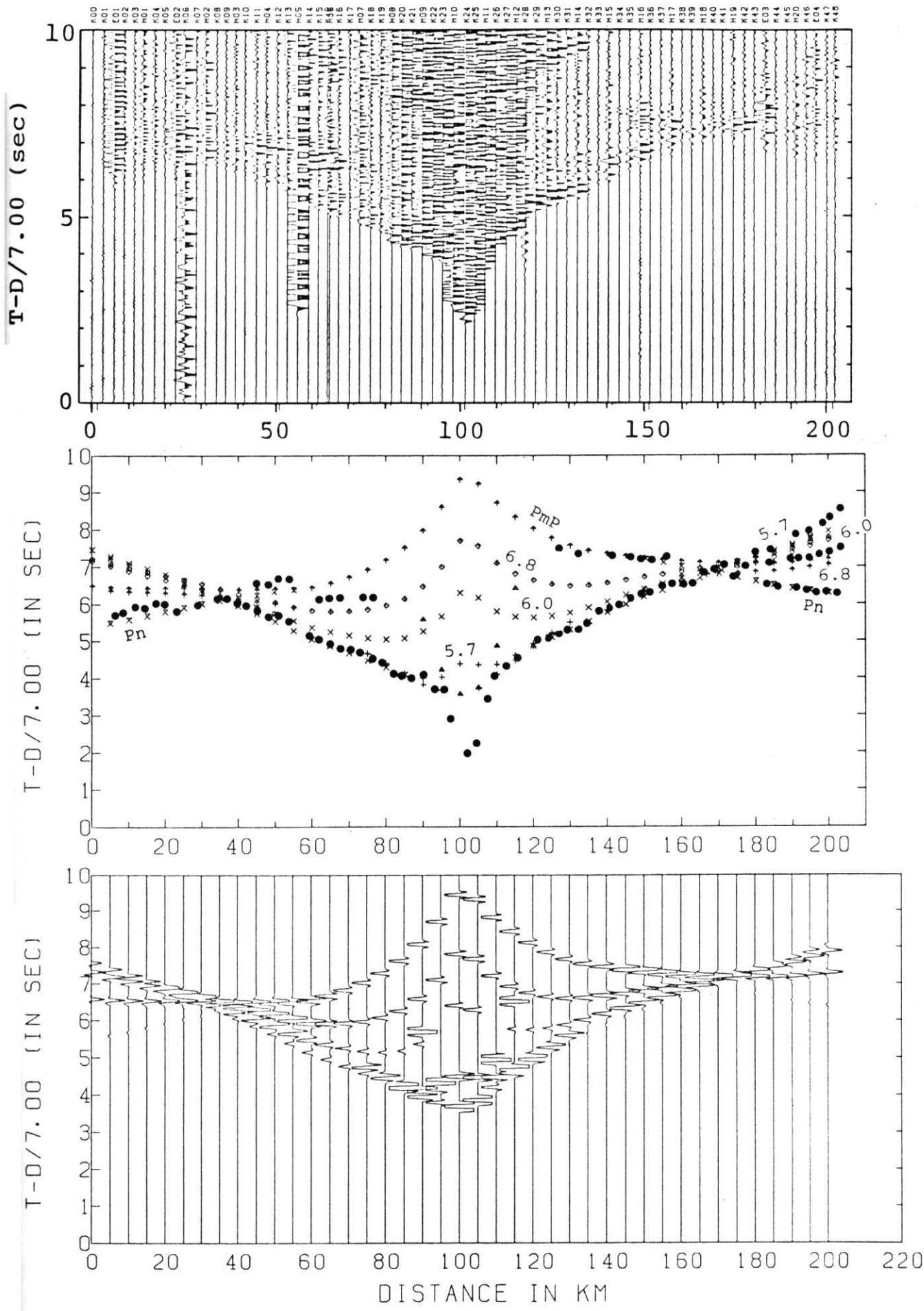
T-D/7.00 (sec)
T-D/7.00 (IN SEC)
T-D/7.00 (IN SEC)
Pn
PmP
6.8
6.0
5.7
Pn
DISTANCE IN KM

FIG. 5.9

# *P7 / PR7*

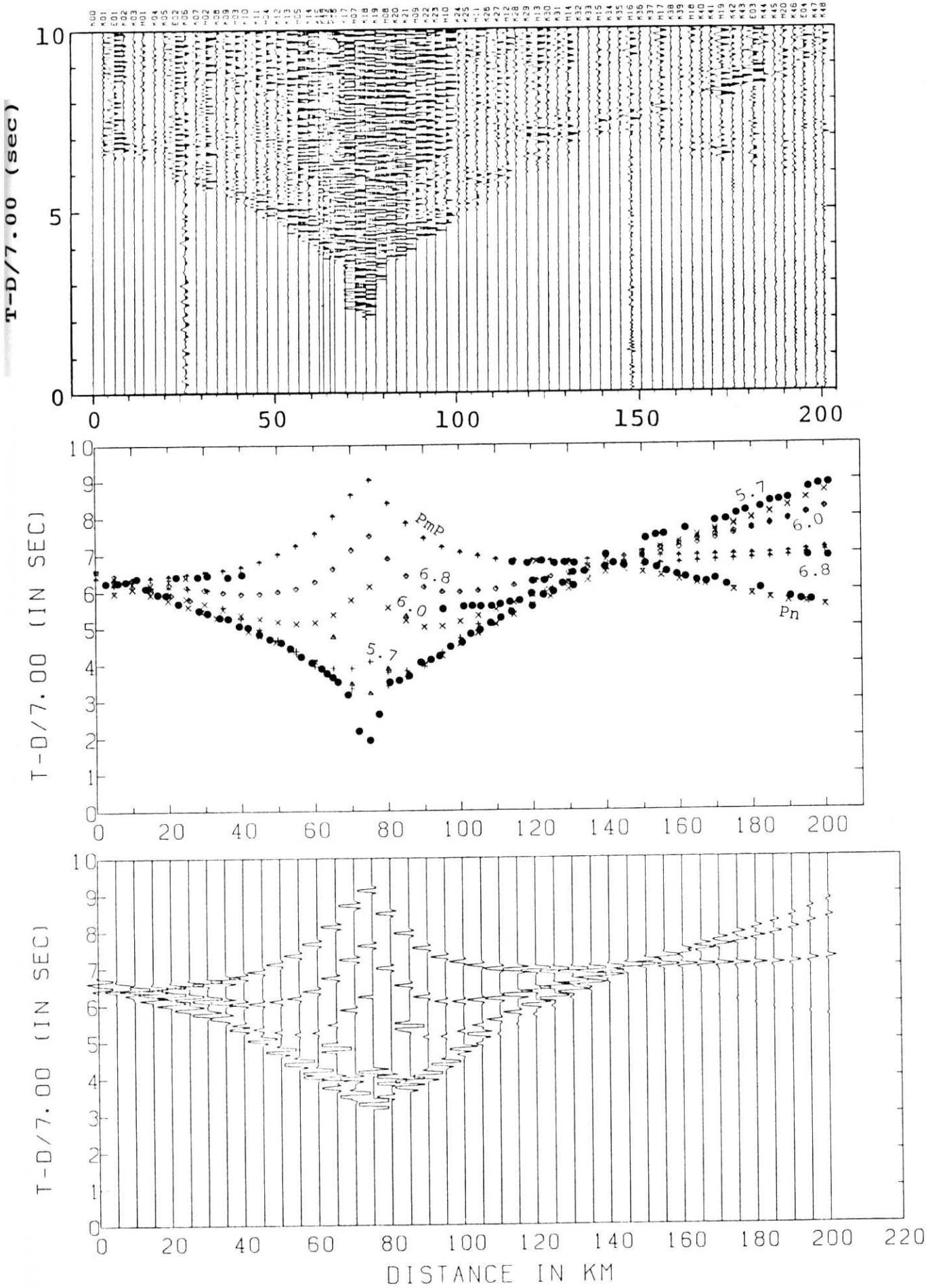


FIG. 5.10

*S9*

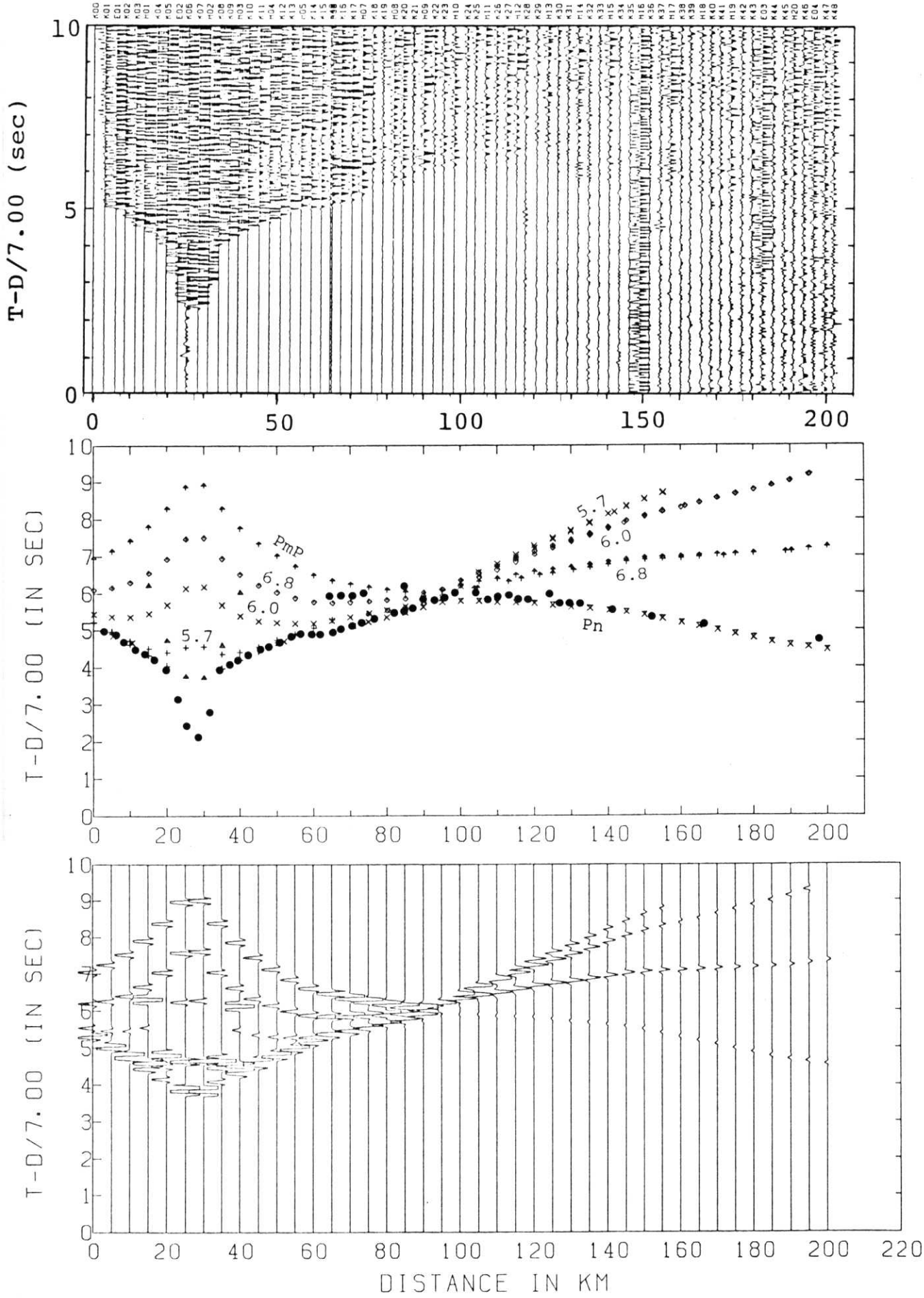


FIG. 5.11

*S10*

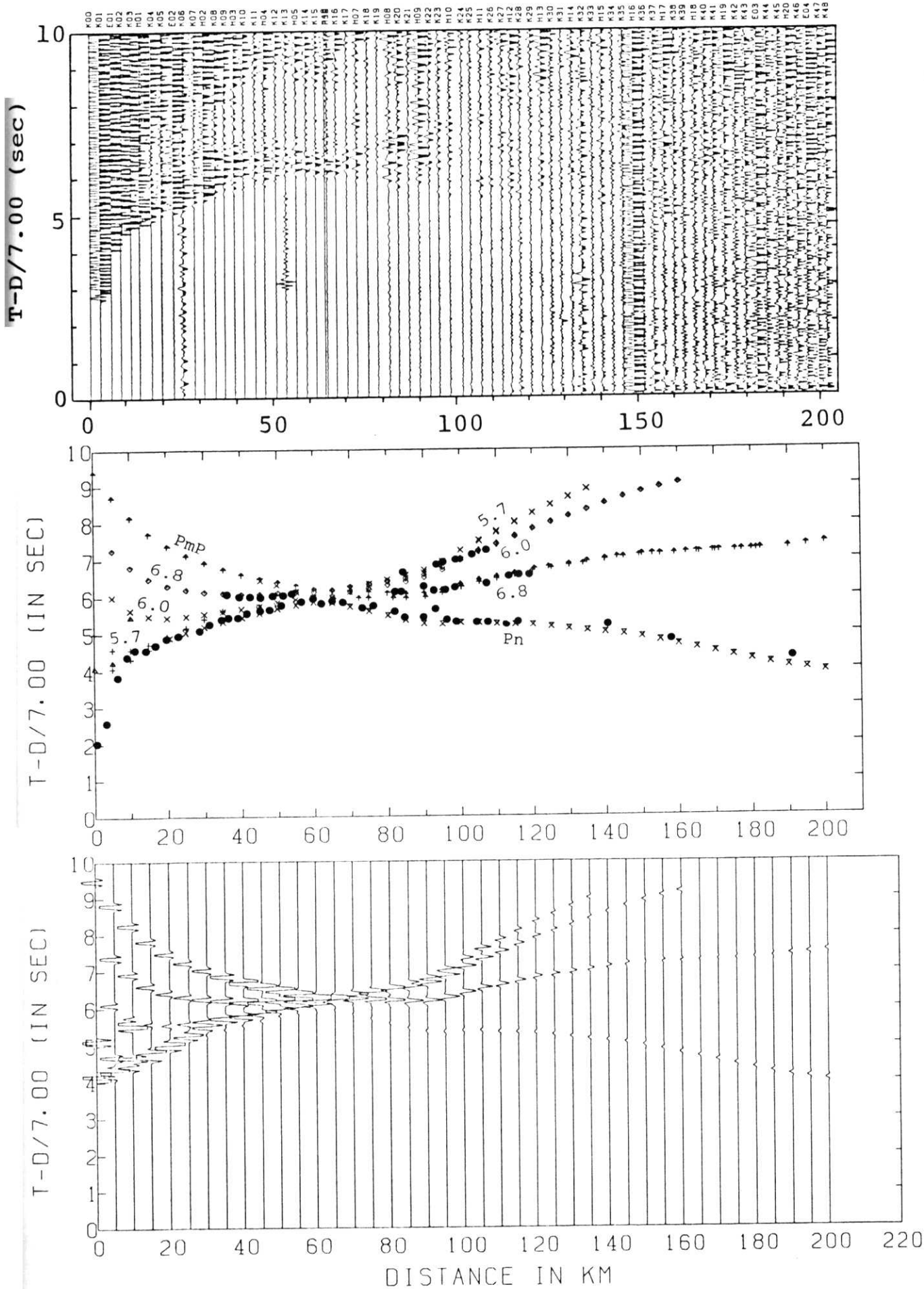


FIG. 5.12

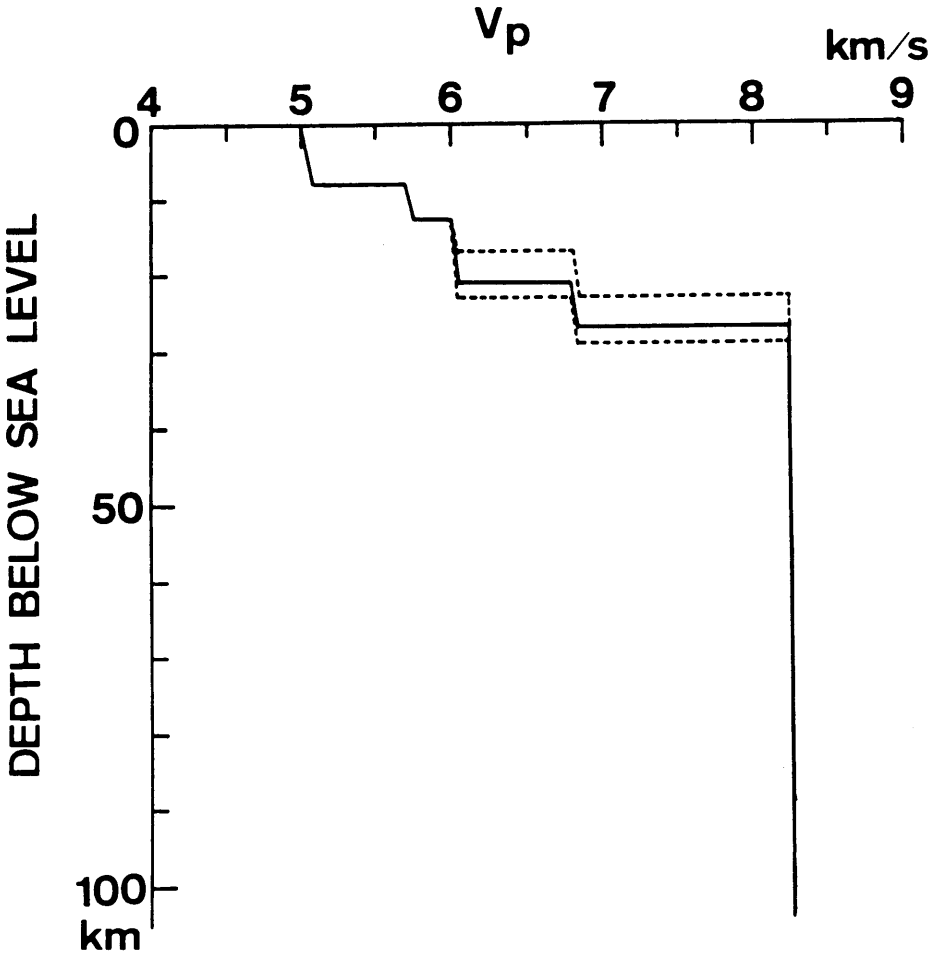


FIG. 5.13

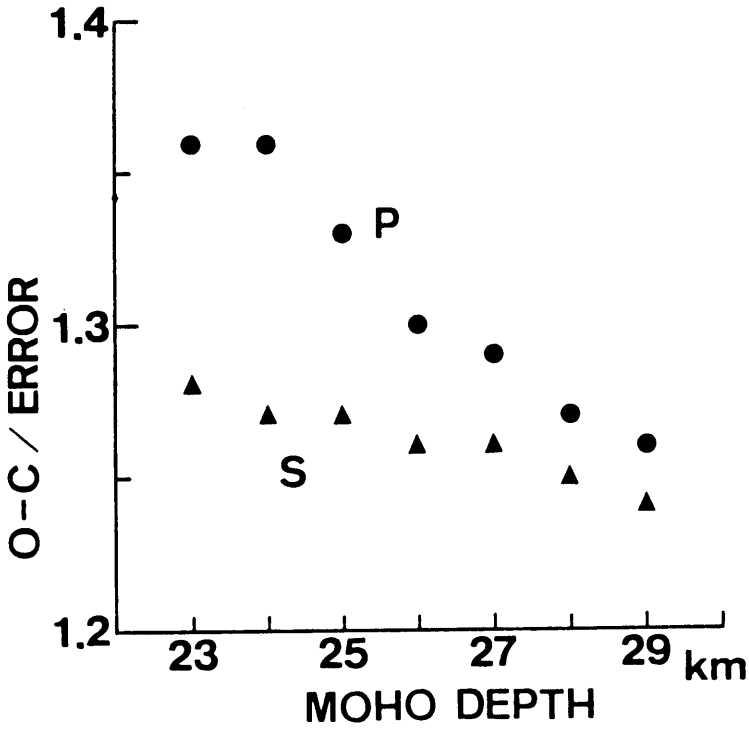


FIG. 5.14

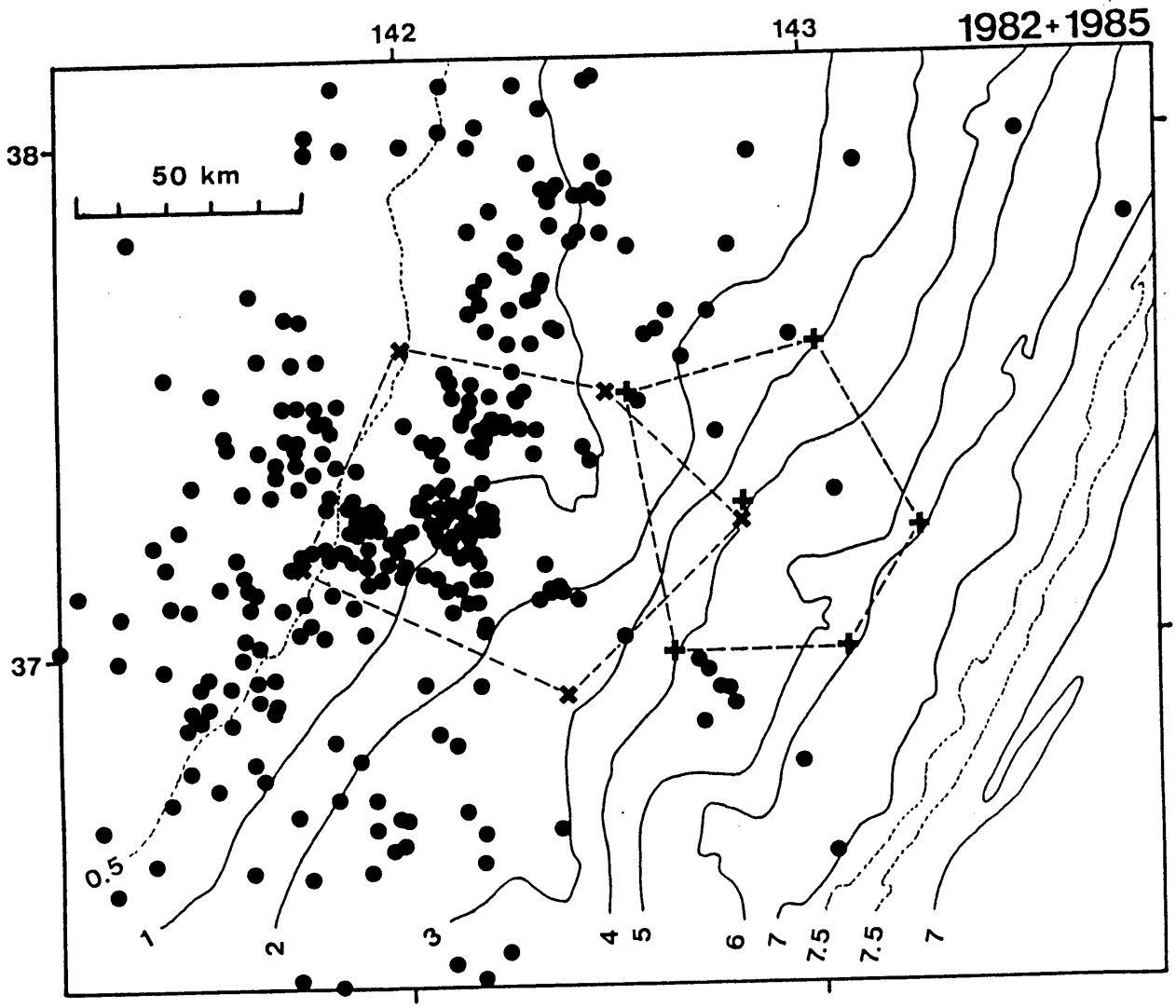


FIG. 5.15

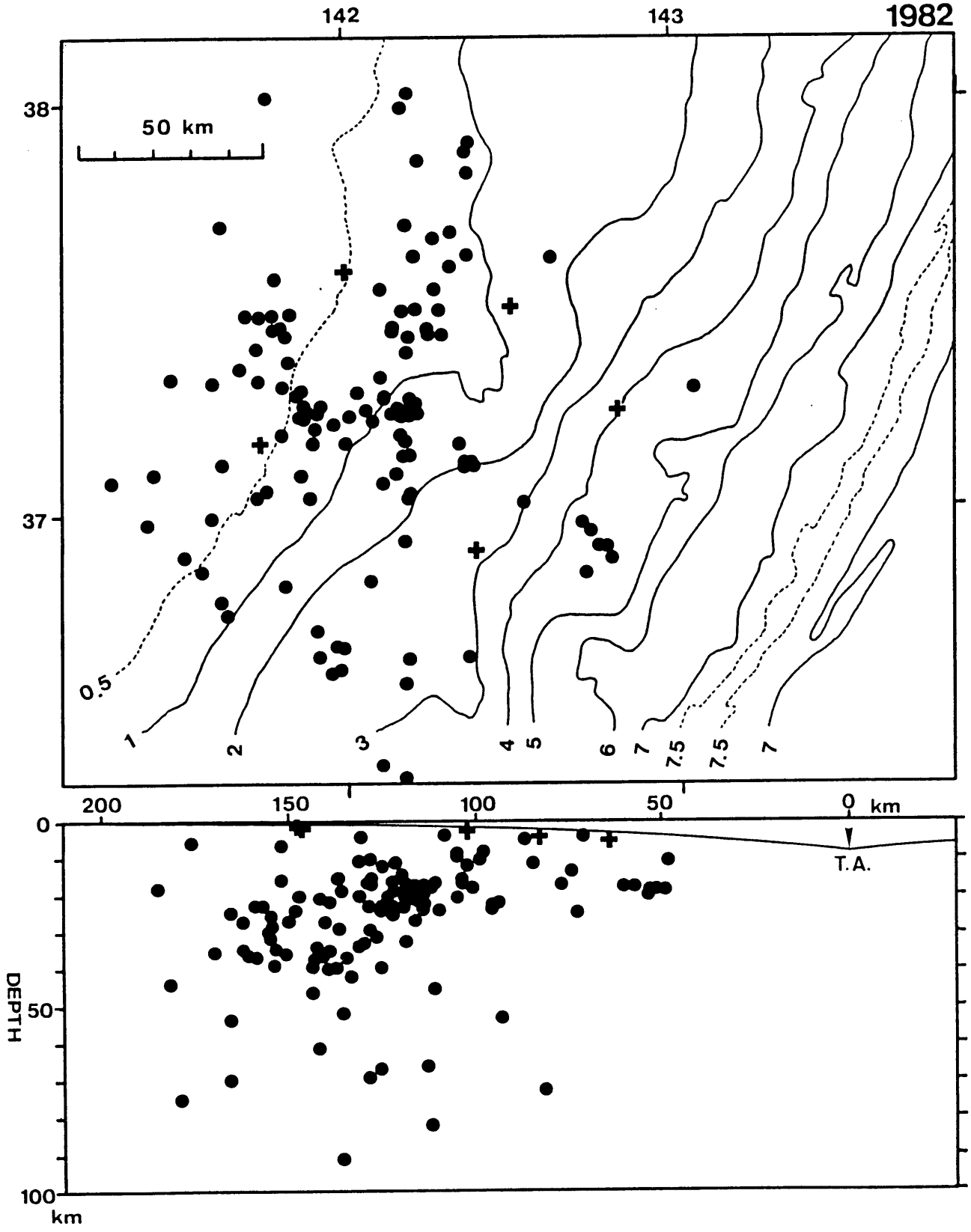
142
143
1982
38
37
50 km
0.5
1
2
3
4
5
6
7
7.5
7.5
7
200
150
100
50
0 km
0
T.A.
DEPTH
50
100
km

FIG. 5.16

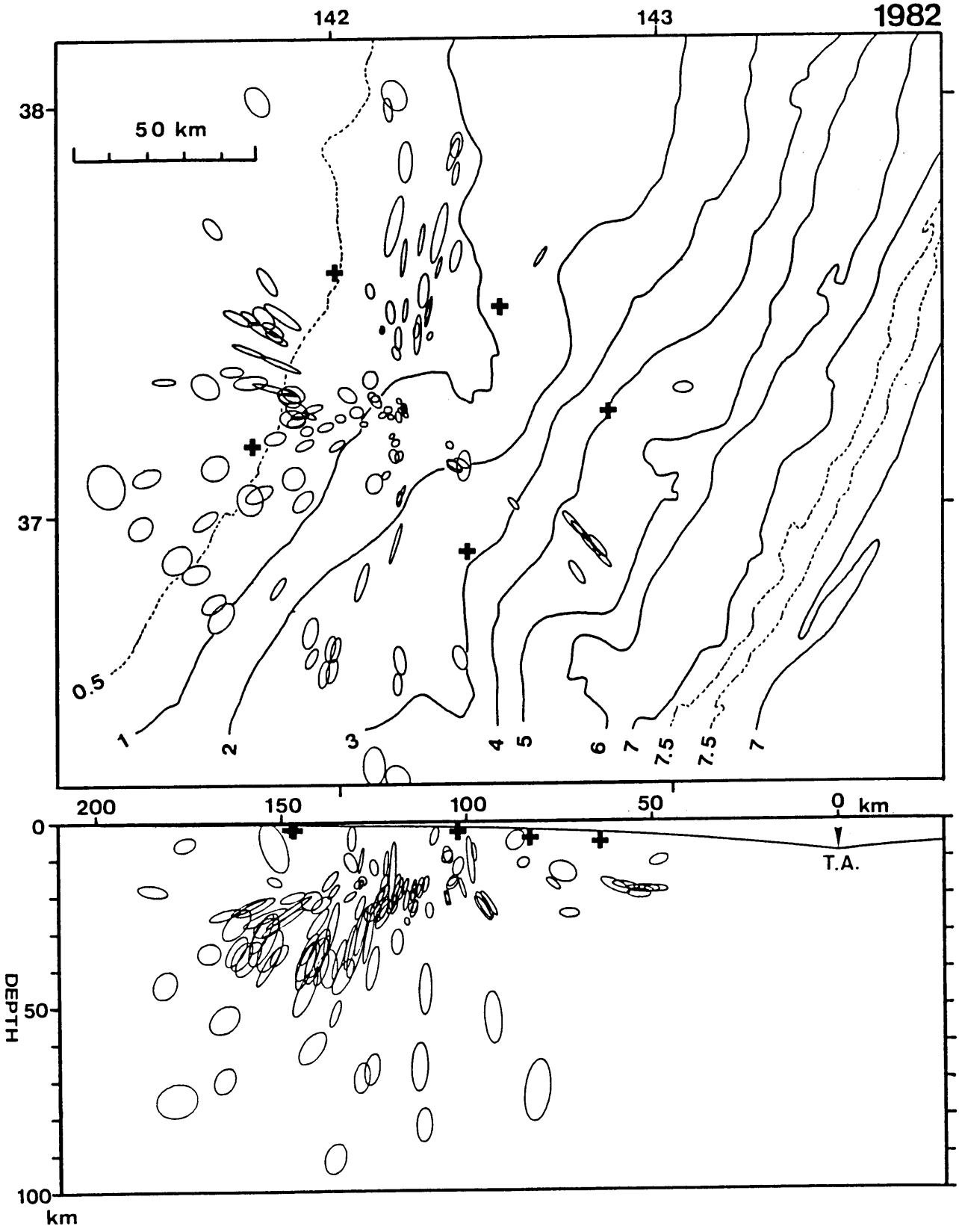
142
143
1982
38
37
50 km
0.5
1
2
3
4
5
6
7
7.5
7.5
7
200
150
100
50
0 km
0
T.A.
DEPTH
50
100
km

FIG. 5.17

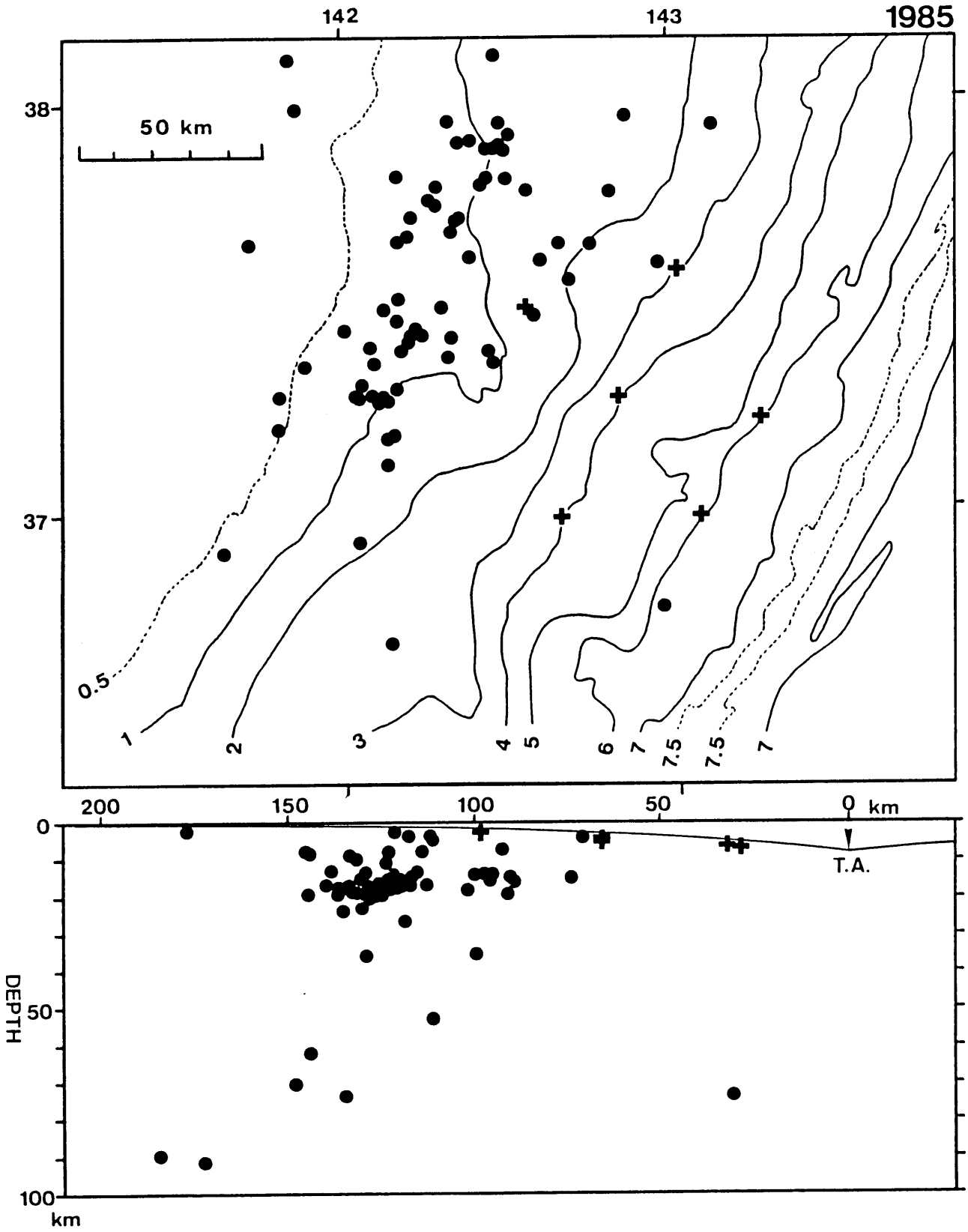
142
143
1985
38
37
50 km
0.5
1
2
3
4
5
6
7
7.5
7.5
7
200
150
100
50
0 km
0
50
100
km
DEPTH
T.A.

FIG. 5.18

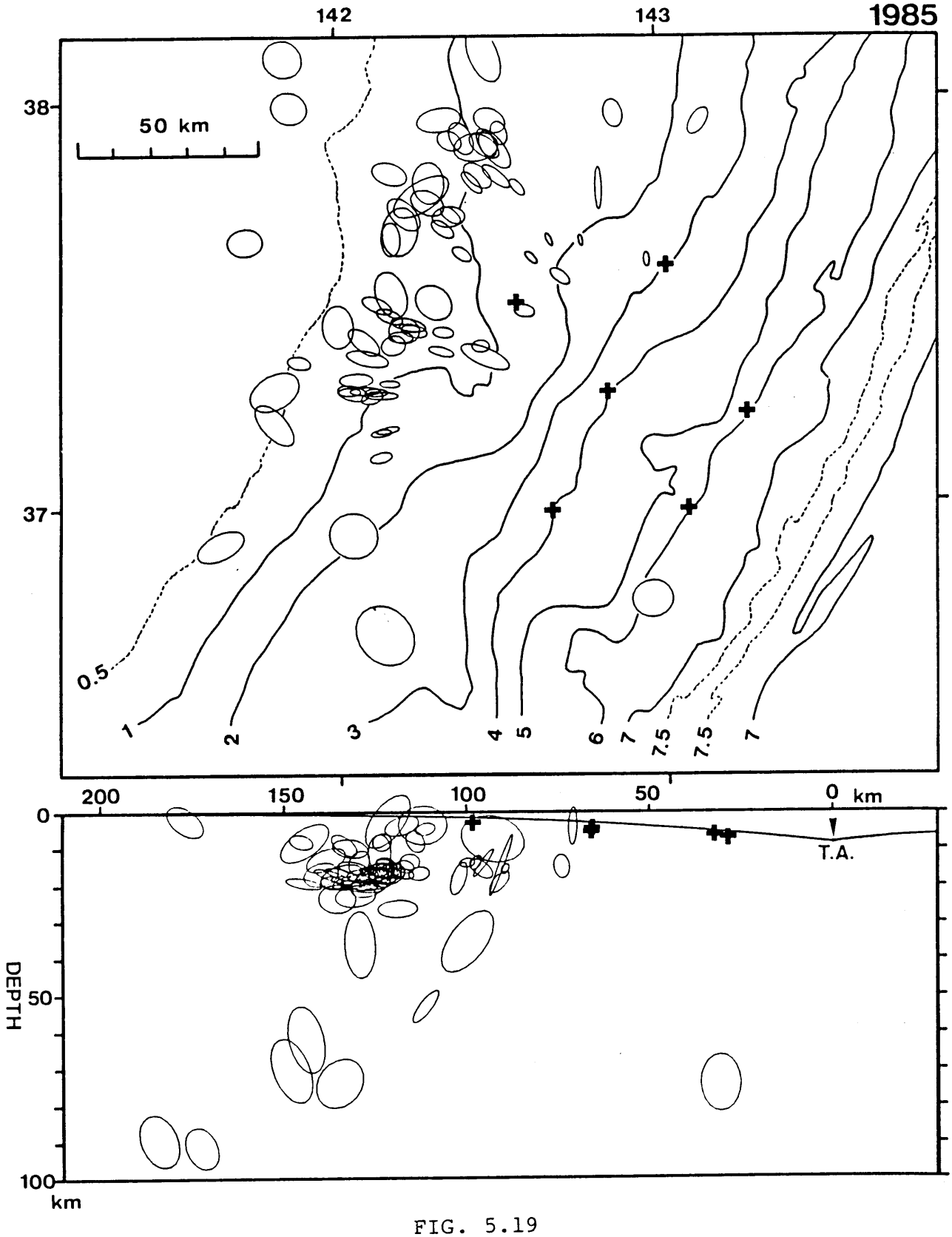
142
143
1985
38
37
50 km
0.5
1
2
3
4
5
6
7
7.5
7.5
7
200
150
100
50
0 km
0
50
100
km
DEPTH
T.A.

FIG. 5.19

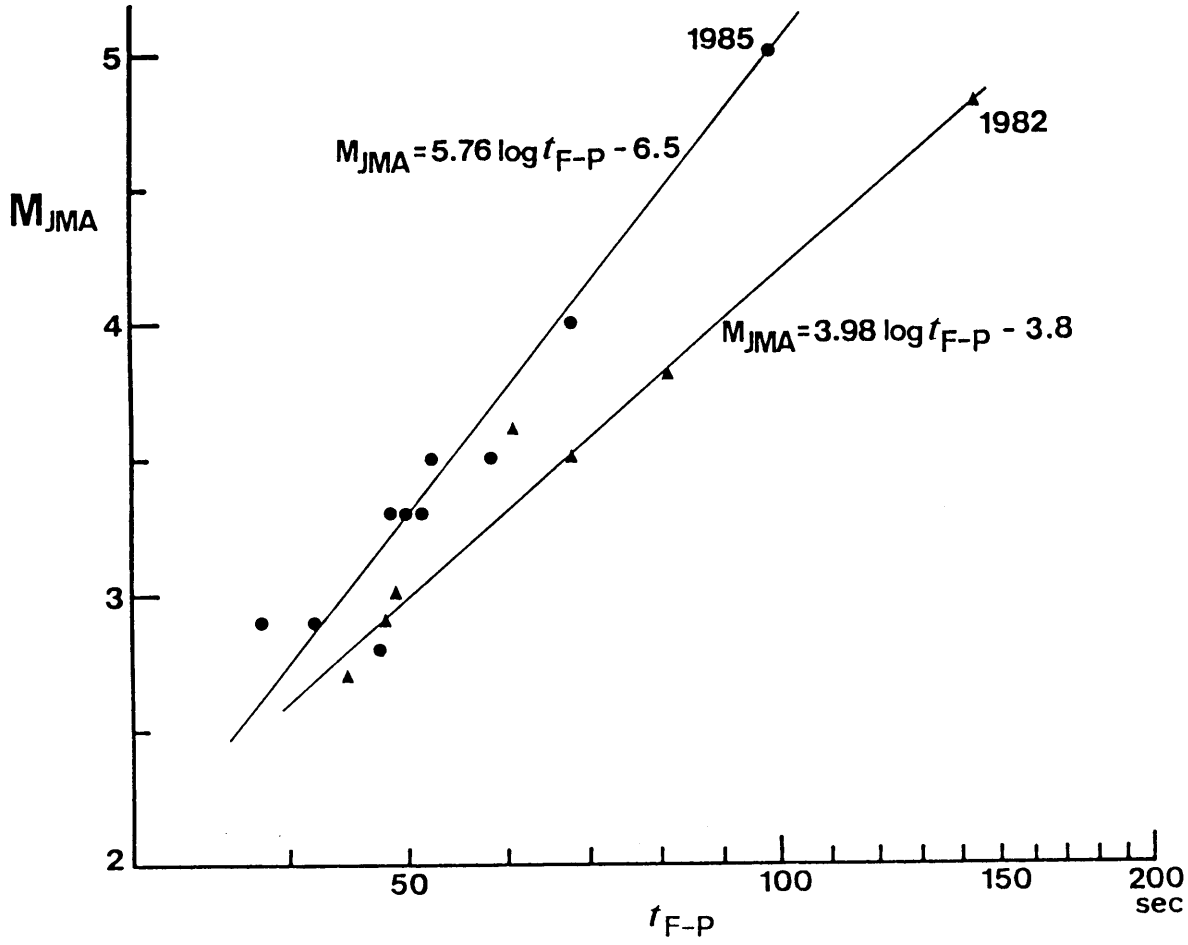
1985
1982
$M_{JMA}=5.76 \log t_{F-P} - 6.5$
$M_{JMA}=3.98 \log t_{F-P} - 3.8$
$M_{JMA}$
5
4
3
2
50
100
150
200
sec
$t_{F-P}$

FIG. 5.20

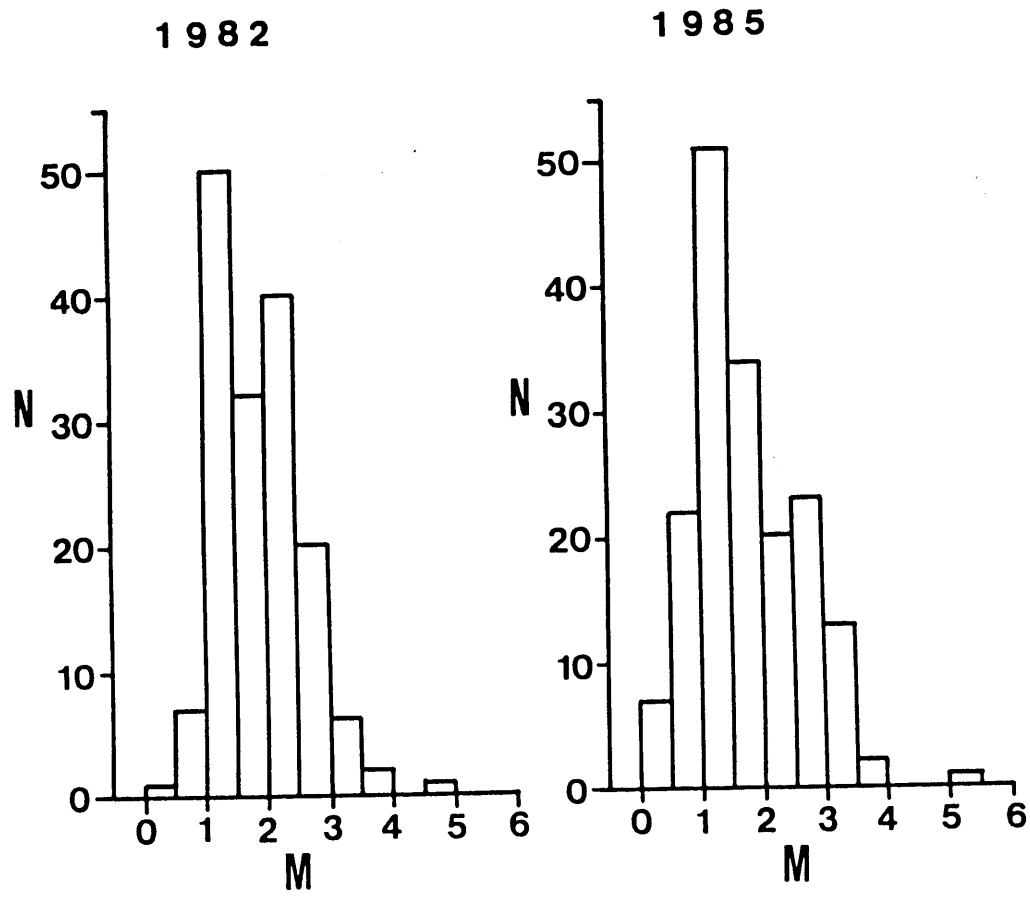


FIG. 5.21

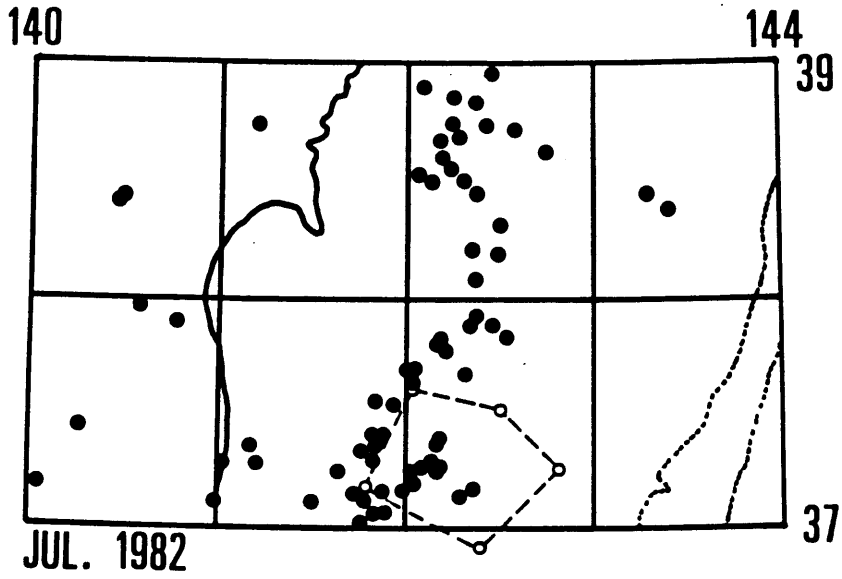


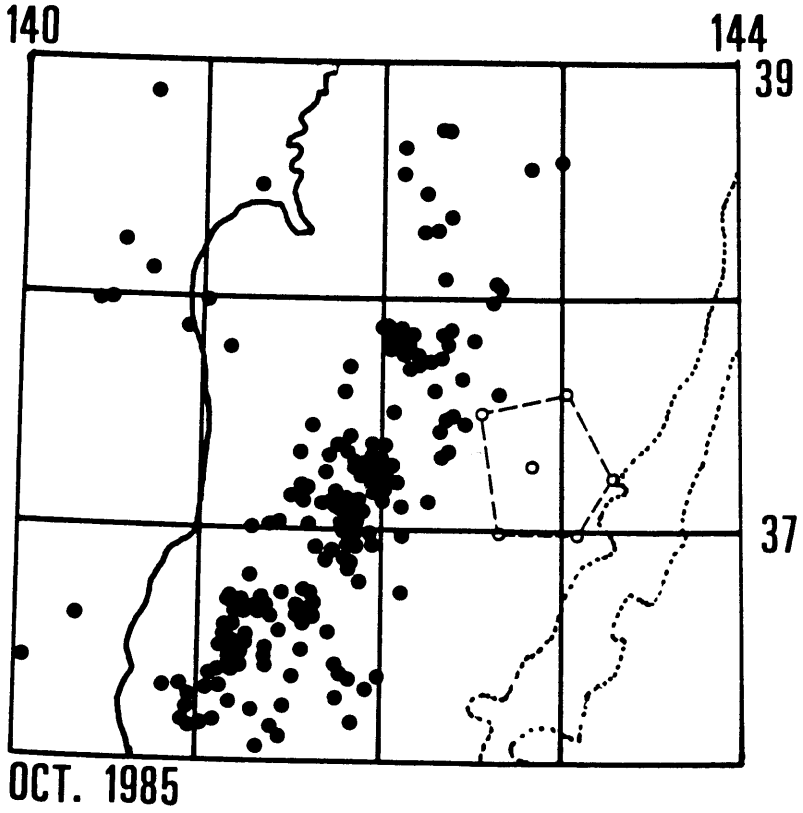


FIG. 5.22

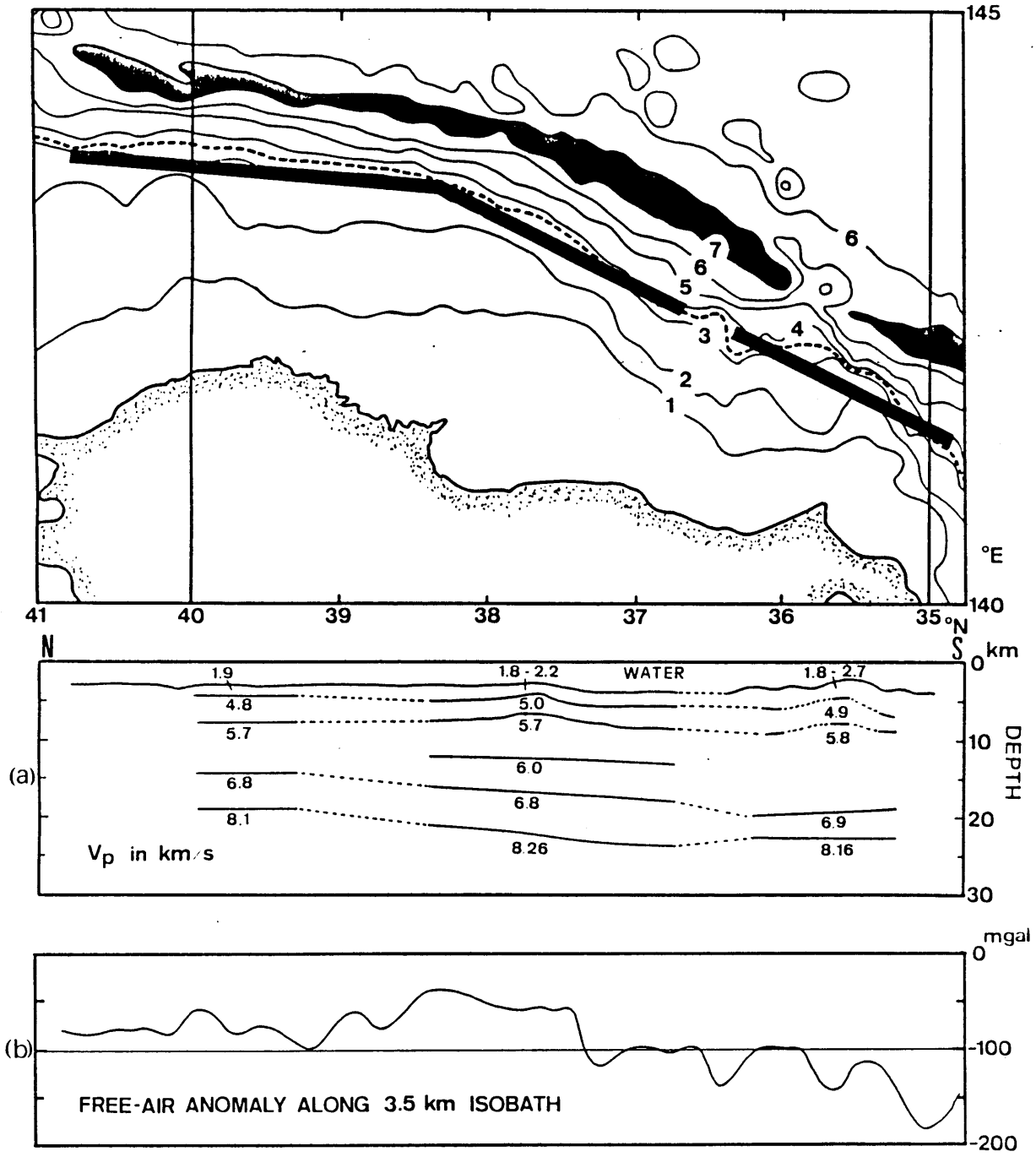
145
°E
140
41
40
39
38
37
36
35 °N
1
2
3
4
5
6
7
N
S
0 km
WATER
1.9
1.8 - 2.2
1.8 - 2.7
4.8
5.0
4.9
5.7
5.7
5.8
6.0
6.8
6.8
8.1
6.9
8.26
8.16
(a)
Vp in km/s
10
20
30
DEPTH
mgal
0
-100
-200
(b)
FREE-AIR ANOMALY ALONG 3.5 km ISOBATH

FIG. 6.1

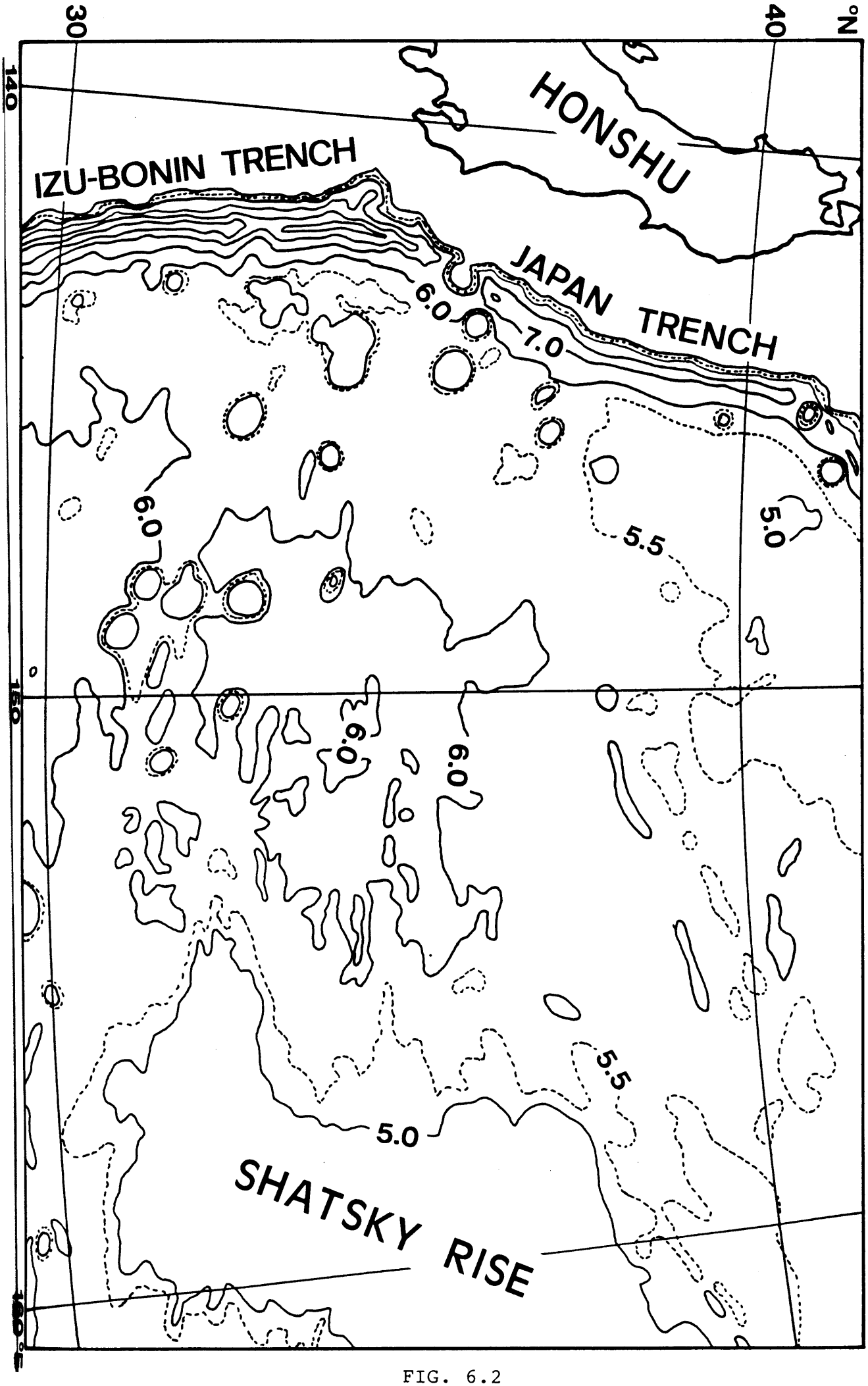
30
40
°N
140
150
160°E
HONSHU
IZU-BONIN TRENCH
JAPAN TRENCH
6.0
7.0
6.0
5.5
5.0
6.0
6.0
6.0
5.5
5.0
SHATSKY RISE

FIG. 6.2

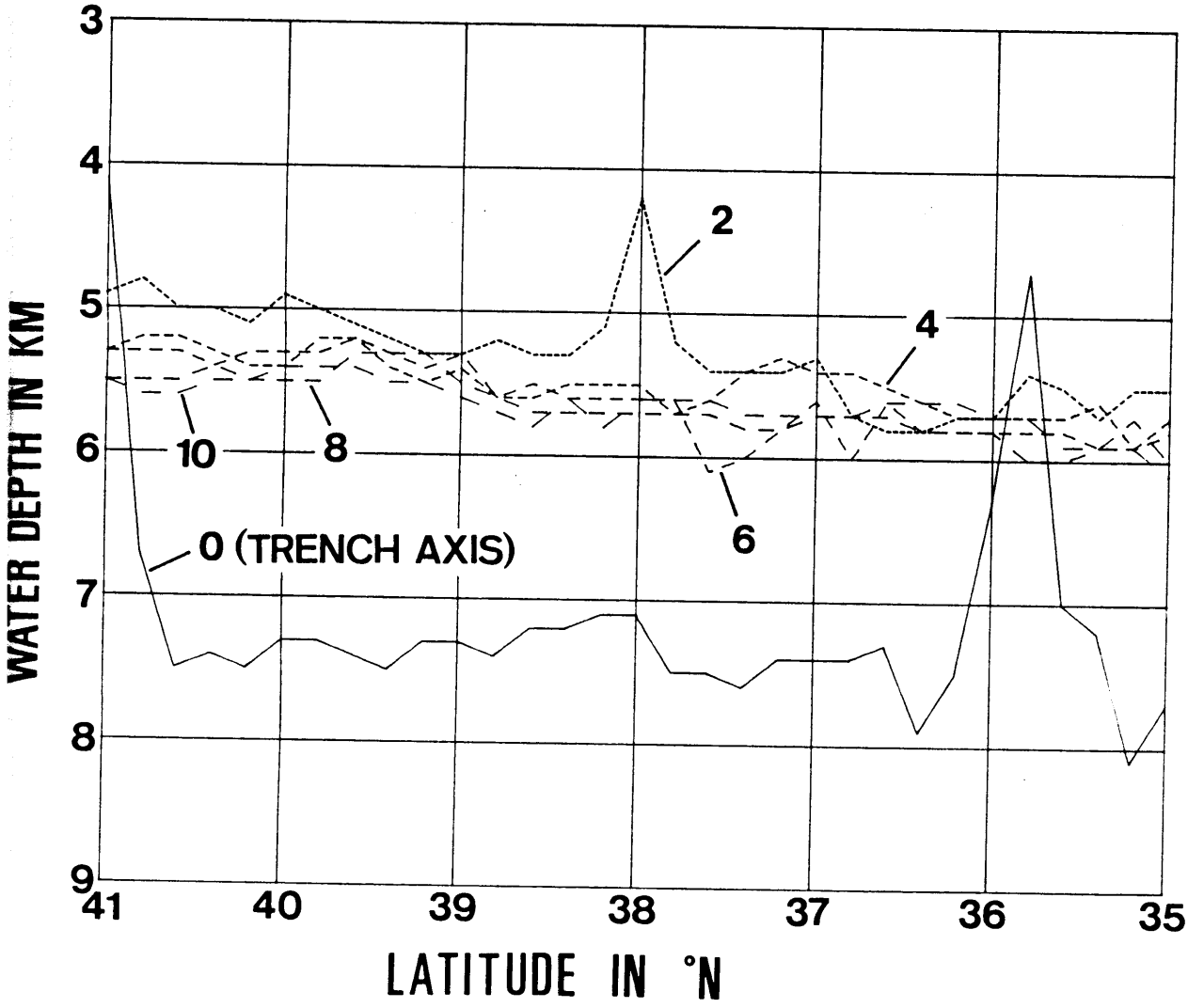
WATER DEPTH IN KM
3
4
5
6
7
8
9
41
40
39
38
37
36
35
LATITUDE IN °N
2
4
10
8
6
0 (TRENCH AXIS)

FIG. 6.3

a)

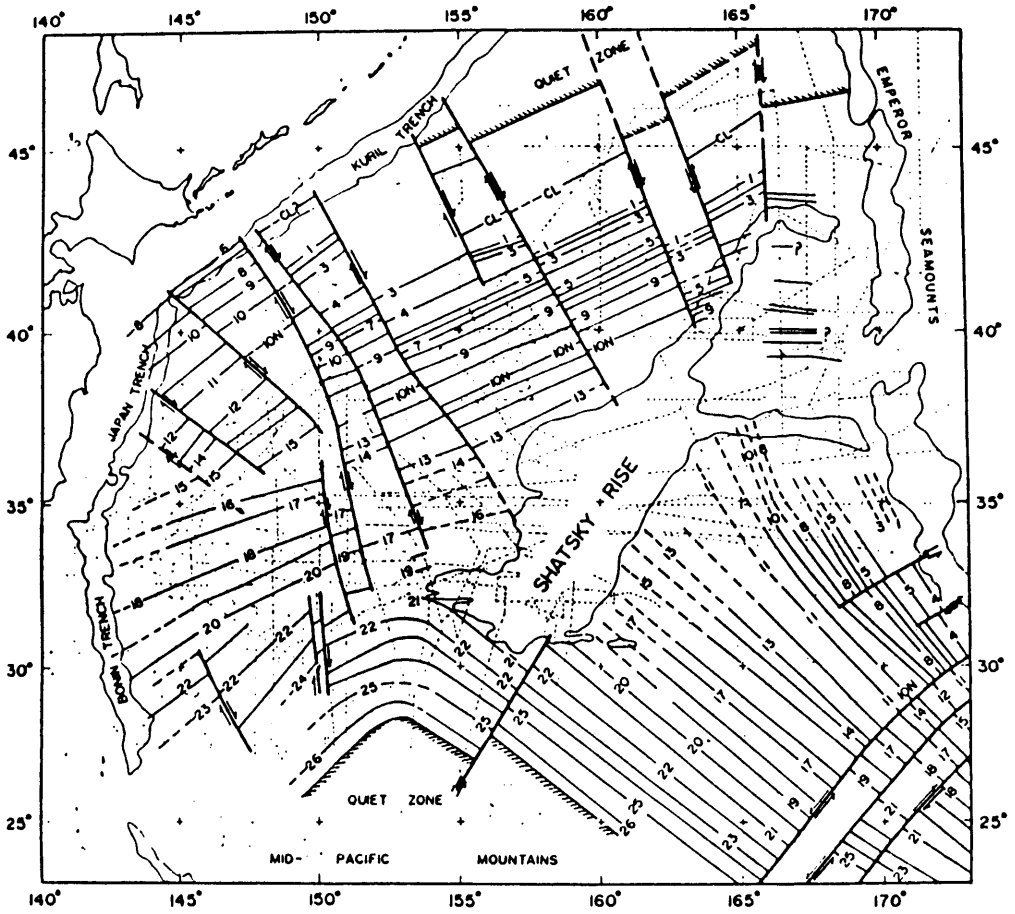
KURIL TRENCH
QUIET ZONE
EMPEROR SEAMOUNTS
JAPAN TRENCH
BONIN TRENCH
SHATSKY RISE
QUIET ZONE
MID- PACIFIC MOUNTAINS
140°
145°
150°
155°
160°
165°
170°
45°
40°
35°
30°
25°

b)

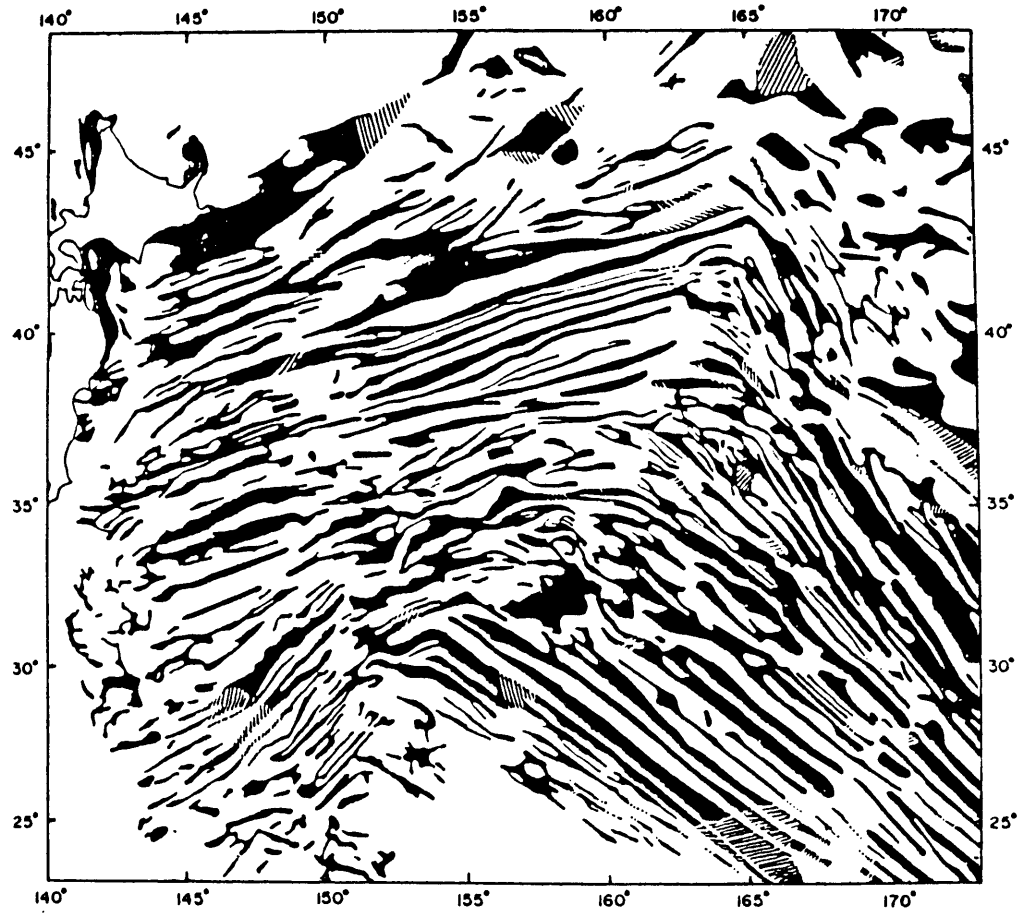
140°
145°
150°
155°
160°
165°
170°
45°
40°
35°
30°
25°

FIG. 6.4

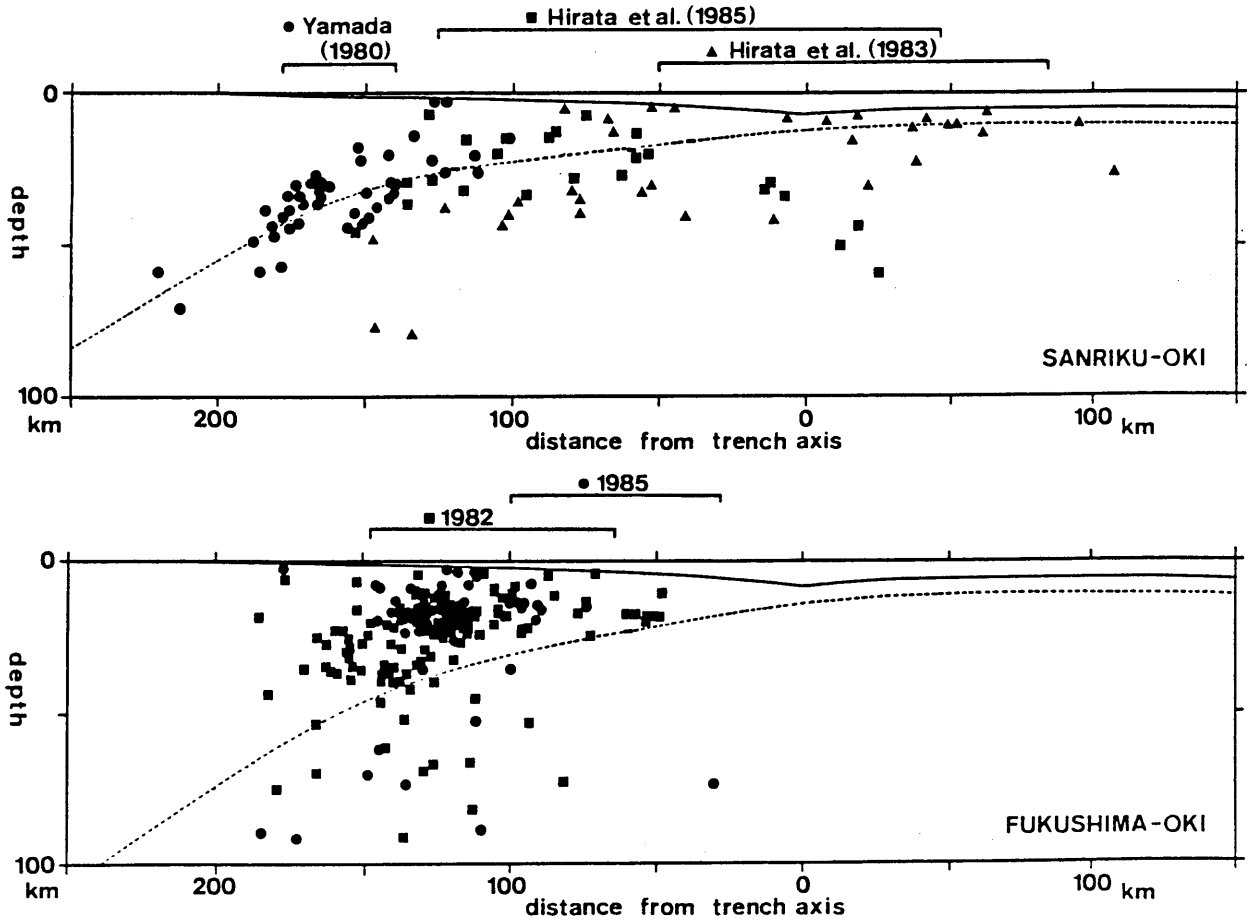
• Yamada (1980)
■ Hirata et al. (1985)
▲ Hirata et al. (1983)
0
depth
100
km
200
100
0
100 km
distance from trench axis
SANRIKU-OKI
• 1985
■ 1982
0
depth
100
km
200
100
0
100 km
distance from trench axis
FUKUSHIMA-OKI

FIG. 6.5